Modeling the Rheological Properties of Plant-based Foods: Soft Matter Principles

David McClements[1]

[1]University of Massachusetts Amherst

May 16, 2023

Abstract

There is growing interest in the design and fabrication of next-generation plant-based (NG-PB) foods that have physicochemical and functional properties that simulate those of traditional animal-based foods, like meat, seafood, egg, and dairy products. Many of these products can be considered as colloidal materials containing particles or polymers that determine their properties, which means that these properties can be understood using soft matter physics concepts. The rheological properties of NG-PB foods may vary widely, including low viscosity fluids (like milk), high viscosity fluids (creams), soft solids (like yogurt), and hard solids (like some cheeses). For manufacturers of NG-PB foods to mimic this broad range of products it is important to have theoretical models to identify, predict, and control the key parameters impacting their textural attributes. In this article, the theoretical models developed to describe the properties of fluid, semi-solid, and solid colloidal dispersions are described, and their potential for improving the design and fabrication of NG-PB foods is highlighted. In the future, it will be important to establish the most appropriate models for different categories of NG-PB foods and to determine their range of applications.

1 **Modeling the Rheological Properties of Plant-based Foods: Soft Matter**

2 **Principles**

3 David Julian McClements*

4 Department of Food Science, University of Massachusetts, Amherst, MA 01003

5

6

7

8

9 *Corresponding author*: David Julian McClements. Department of Food Science, University

10 of Massachusetts, Amherst, MA 01003, USA. Tel: 413 545 2275; email: mcclemen@umass.edu

11

12

Abstract

There is growing interest in the design and fabrication of next-generation plant-based (NG-PB) foods that have physicochemical and functional properties that simulate those of traditional animal-based foods, like meat, seafood, egg, and dairy products. Many of these products can be considered as colloidal materials containing particles or polymers that determine their properties, which means that these properties can be understood using soft matter physics concepts. The rheological properties of NG-PB foods may vary widely, including low viscosity fluids (like milk), high viscosity fluids (creams), soft solids (like yogurt), and hard solids (like some cheeses). For manufacturers of NG-PB foods to mimic this broad range of products it is important to have theoretical models to identify, predict, and control the key parameters impacting their textural attributes. In this article, the theoretical models developed to describe the properties of fluid, semi-solid, and solid colloidal dispersions are described, and their potential for improving the design and fabrication of NG-PB foods is highlighted. In the future, it will be important to establish the most appropriate models for different categories of NG-PB foods and to determine their range of applications.

Keywords: soft matter physics; rheology; plant-based foods; colloidal dispersions; nanoparticles; biopolymers

1. Introduction

In this article, the term "next-generation plant-based (NG-PB) foods" is used to refer to foods formulated from plant-derived ingredients, such as lipids, proteins, and polysaccharides, that are specifically designed to mimic the properties of animal sourced foods like meat, seafood, eggs, and dairy products [1]. The focus of this article is on understanding, predicting, and controlling the rheological characteristics of NG-PB foods, like the flowability of milk and cream analogs or the hardness of meat, egg, and cheese analogs [2]. Rheological attributes like shear viscosity (for fluids) and elastic modulus and fracture properties (for solids) influence the processing, quality, shelf life, and sensory attributes of NG-PB foods [1, 3]. It is therefore important to understand the factors that contribute to the rheology of this category of foods, as this enables food designers and manufacturers to create products with the rheological attributes required for their intended

43 application. The rheological properties of materials depend on how they flow or deform when a

44 particular type of stress is applied to them, such as a normal, shear, and/or extensional stress [4].

45 NG-PB foods exhibit a wide range of rheological characteristics depending on their compositions

46 and processing. For instance, NG-PB milks are typically low viscosity liquids, NG-PB sauces

47 and dressings are viscous fluids, NG-PB yogurts and eggs are soft gels, and NG-PB cheddar

48 cheese and cooked meat are hard gels [1]. Even within a particular rheological category, the

49 properties of NG-PB foods can vary considerably. For instance, the fracture properties of solid

50 NG-PB foods may range from hard and brittle to soft and malleable, which is important for

51 determining their mouthfeel and other sensory qualities.

52 NG-PB foods span the whole range of materials normally covered by soft matter physics, and

53 so the principles of this discipline can be employed to better understand and control their

54 properties [5-7]. The majority of NG-PB foods are primarily comprised of colloidal particles and

55 polymers, which play a critical role in determining their overall rheological attributes. These

56 colloidal particles include oil bodies, oil droplets, protein particles, starch granules, and plant

57 tissue fragments, while the polymers include polysaccharide and protein molecules, as well as

58 their assemblies [1]. The main focus of this article is to outline the current understanding of

59 colloidal and polymer dispersions, with an emphasis on providing physical concepts and

60 theoretical models describing their properties. These concepts and models should improve our

61 understanding of the factors that impact the rheology of NG-PB foods, which should facilitate

62 the design and fabrication of better-quality products.

63 ## 2. Plant-based Foods as Colloidal Dispersions

64 As mentioned in the introduction, the majority of NG-PB foods can be considered to be

65 colloidal dispersions consisting of small particles and/or polymer molecules suspended in an

66 aqueous matrix (**Figure 1**). In this section, we provide a brief overview of the different kinds of
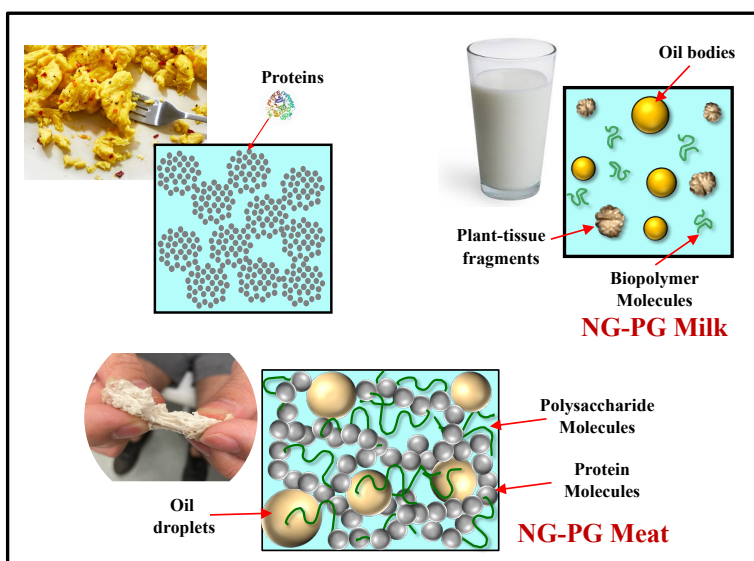
67 these products.

Figure 1. Schematic diagram of the importance of colloids and polymers in selected NG-PB food products. Proteins, polysaccharides, oil bodies, and oil droplets are all examples of colloidal materials found in these soft-matter foods.

2.1. NG-PB dairy products: Milk, cream, yogurt, and cheese

NG-PB milks are complex colloidal dispersions containing several kinds of particles or polymers suspended in an aqueous solution, which may also contain dissolved substances like sugars and salts [8, 9]. For instance, they may contain oil bodies, oil droplets, plant cell fragments, protein aggregates, and/or polysaccharides dispersed in water (**Figure 1**). These products typically have a relatively low viscosity that is designed to simulate the low viscosity of cow's milk [9]. However, in some cases, thickening agents (such as gums) are added to inhibit the creaming or sedimentation of the colloidal particles they contain, which leads to a pronounced increase in their viscosity [10, 11]. Structurally, NG-PB creams are similar to NG-PB milks, but the fat content is higher, which leads to a higher viscosity (see later). NG-PB yogurts are soft gels whose rheological properties are dominated by the present of a 3D network of aggregated biopolymers, usually formed from added proteins, starches, and/or gums, or by polymers secreted during microbial fermentation [12]. NG-PB cheeses are semi-solid materials that may vary from relatively soft gels (like Brie) to hard gels (like cheddar) [13, 14]. The rheological properties of these materials are also dominated by a 3D network of biopolymer molecules, but the presence of fat droplets and/or a fat crystal network may also contribute to their texture and mouthfeel.

2.2. NG-PB meat and seafood products

NG-PB meat and seafood products are often designed to have a fibrous microstructure that mimics those found in the equivalent animal products [15]. Food manufacturers aim to simulate this kind of microstructure because it influences the desirable textural and mouthfeel attributes of the end product. Often this kind of fibrous structure is created by using an appropriate blend of proteins and polysaccharides (**Figure 1**). Some of the most common proteins used to formulate commercial NG-PB meat and seafood products include those isolated from soybeans, peas, rice, mung beans, faba beans, and wheat proteins, while some of the most common polysaccharides include starch, methylcellulose, and various gums. Fibrous structures are typically formed using mechanical methods, such as extrusion or shear cell technology [3, 16], but it can also be created using soft matter physics approaches, such as phase separation-shearing-gelation methods [1]. Fibrous structures are usually formed using proteins and/or polysaccharides as structure-forming elements [16]. There has also been interest in creating NG-PB adipose tissue to simulate the adipose tissue found in real meat and seafood products. For instance, highly concentrated oil-in-water emulsions fabricated from plant or microbial fats, proteins, and polysaccharides have been developed as NG-PB adipose tissue analogs to mimic the whitish appearance and solid-like texture of real adipose tissue [17-19]. Some of the plant-based versions have even been designed to simulate the melting and crystallization of real adipose tissue. In an alternative approach, liquid plant-derived oils have been converted into solid fats using enzyme glycerolysis, which led to products that exhibited similar characteristics as high-melting animal fats [20]. Oleogels and emulsion gels formulated from plant-derived ingredients have also been developed recently to replace the fats in meat and seafood products [21].

Typically, NG-PB meat and seafood products are semi-solid materials whose hardness and fracture properties are designed to simulate those found in the real animal sourced products they are intended to replace. From a rheological point of view, they can be considered to consist of filled polymer gels that contain fibers and particles (**Figure 1**).

2.3. NG-PB egg and egg products

NG-PB egg analogs are typically colloidal dispersions containing particles (like oil droplets) and polymers (like proteins and/or polysaccharides) (**Figure 1**) [1, 22]. Commercially, they may be sold in a fluid or solid form. In the fluid form, they are usually viscous fluids that form gels when they are heated during cooking, such as frying or baking. The initial viscosity of fluid NG-

121   PB eggs needs to be relatively high to prevent creaming or sedimentation of any particulate

122   matter during storage, such as fat droplets, starch granules, or protein aggregates. During

123   heating, gelation usually occurs as a result of the unfolding and aggregation of globular plant

124   proteins, which leads to the formation of a 3D protein network that provides elastic properties [23].

125   Ideally, gelation should begin at the same temperature as for real eggs (around 65 to 70 °C) and

126   the gels formed should have similar textural attributes to real eggs. In the solid form, NG-PB egg

127   products may be sold in a pre-gelled state that mimics the properties of cooked egg, like egg

128   slices that can be cooked in a microwave, toaster, or frying pan.

129   Egg analogs may also be used to create other products that real eggs are typically used for,

130   such as plant-based salad dressings or mayonnaises [24]. These products are concentrated oil-in-

131   water emulsions that typically have a yield stress and a high viscosity. These semi-solid

132   characteristics may arise for several reasons, including the fact that the oil droplets are closely

133   packed together in concentrated systems, the oil droplets may be aggregated with each other, or

134   thickening or gelling agents (like gums or starches) are added.

3. Colloidal Dispersions

136   In this section, we highlight the main characteristics of the particles and polymers present in

137   the colloidal dispersions that might be found in NG-PB foods that may influence their

138   rheological properties. Typically, it is important to identify the different kinds of particles and

139   polymers present, as well as to have knowledge of their molecular and physicochemical

140   properties, as this influences the processing, shelf life, quality attributes, and sensory properties
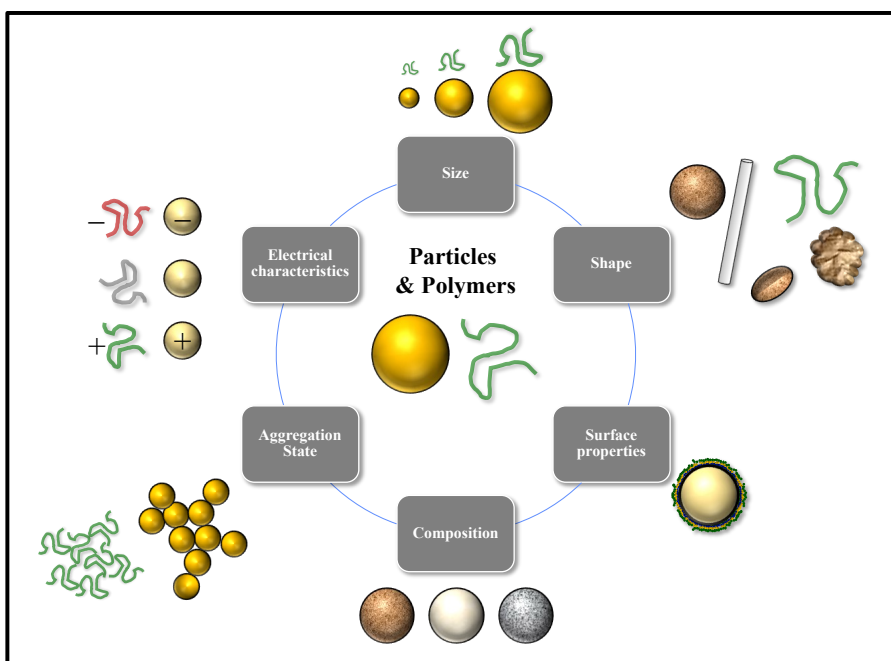
141   of these foods.

Figure 2. The properties of the particles and polymers in NG-PB foods varies, which alters their rheological properties.

3.1. Particles

Colloidal particles vary in their compositions, sizes, shapes, polarities, charges, interactions, and aggregation states (**Figure 2**), which determines their impact on the rheology of NG-PB foods. In general, the properties of colloidal particles impact the rheology of both fluid and solid foods, which can often be described by theoretical equations or computational models [4].

Composition: The particles in NG-PB foods may be comprised of different edible substances depending on their origin and processing, including proteins, polysaccharides, lipids, phospholipids, minerals, and their combinations [1, 15]. For instance, the oil bodies present in many oil-rich plant materials (such as nuts and beans) consist of a triacylglycerol core surrounded by a layer of phospholipids with proteins embedded in it [25, 26]. These oil bodies may be present in NG-PB milks created using top-down methods that utilize size-reduction operations to disrupt plant tissues and release the oil bodies [9]. The oil droplets in NG-PB milks formulated using bottom-up methods, like homogenization of oil, water, and emulsifier, typically consist of a triacylglycerol core surrounded by a layer of emulsifier molecules (often proteins, polysaccharides, phospholipids, and/or saponins) [9]. In their natural state, raw starch granules consist of a mixture of amylose and amylopectin molecules organized into amorphous and

7

162 crystalline regions [27]. During processing and cooking, the raw starch granules absorb water and

163 swell (gelatinize), which changes their composition and functional attributes. Some NG-PB

164 foods, such as milk and cheese analogs, are created from comminated plant materials (such as

165 nuts or seeds), and therefore contain plant tissue fragments, including cell wall materials rich in

166 dietary fibers [28]. NG-PB meat, seafood, and egg products often contain protein assemblies, such

167 as fibers or particulates, that vary considerably in their length scales (**Figure 2, Table 1**). These

168 assemblies can be formed from many different kinds of plant proteins, including those isolated

169 from soy, corn, wheat, pea, mung bean, and potato. Identification of the various kinds of

170 colloidal particles in a NG-PB food is important because they influence its rheological

171 properties.

172 *Particle size and shape*: The particles in NG-PB foods may vary considerably in their sizes

173 and shapes (**Figure 2**). For instance, their dimensions may range from a few nanometers (small

174 protein aggregates) to a few millimeters (texturized vegetable proteins), which covers around six

175 orders of magnitude in length scale. The oil bodies or oil droplets in NG-PB milks and creams

176 typically vary from around 100 to 5000 nm [9]. The protein particles formed when globular plant

177 proteins are heated above their thermal denaturation temperature may also vary from around 100

178 to 5000 nm depending on protein type, protein concentration, solution conditions, and processing

179 conditions [29, 30]. Raw starch granules may vary in size from below a micrometer to above 100

180 micrometers depending on the species and maturity of the plant source, as well as the growing

181 conditions [31]. Gelatinized starch granules are considerably larger than raw ones because they

182 absorb water from their surroundings when they are heated and swell [32]. Plant tissue fragments

183 may vary considerably in dimensions (from micrometers to millimeters) depending on the

184 method used to breakdown the original plant materials, such as mechanical, chemical, or

185 enzymatic methods [28]. Texturized vegetable proteins are typically designed to be a few

186 millimeters in size to mimic the dimensions of the pieces found in comminuted meat products [33].

187 Mechanical size-reduction methods like milling, grinding, and homogenization may be used to

188 reduce the particle size of plant tissues to inhibit gravitational separation in products like plant-

189 based eggs and milk, or to improve the mouthfeel by removing large particles that would give a

190 gritty or rough feeling like in plant-based milks and creamers. Enzyme treatments using

191 proteases, amylases, cellulases, hemicellulases, or pectinases are sometimes used to reduce the

192 size of starch granules, protein particles, or plant-tissue fragments for similar reasons.

193   The shape of the particles in NG-PB foods may also vary considerably (**Figure 2**). Oil

194   bodies, oil droplets, starch granules, and colloidal protein aggregates are often spherical or

195   spheroidal. However, protein aggregates and plant tissue fragments may have fibrous or

196   irregular shapes. For instance, NG-PB meat or seafood products often contain protein or

197   polysaccharide aggregates or domains that have fibrous structures, because this better simulates

198   the textural attributes and mouthfeel of real products [2, 3]. These fibrous structures can be

199   produced using processing methods (like extrusion or shear cells) or physicochemical methods

200   (like phase separation, shearing, and gelling).

201   In general, the size and shape of the colloidal particles within NG-PB foods have a large

202   impact on their textural attributes. For instance, particles larger than about 50 μm can be

203   detected as discrete objects within the human mouth, which may be undesirable in products

204   where a smooth mouthfeel is required (like plant-based milks and creams) but desirable in

205   products where a more textured mouthfeel is desirable (like plant-based burgers or sausages).

206   The size and shape of food particles also influence their ability to form 3D networks, which

207   influences the textural attributes of semi-solid and solid NG-PB foods, like meat, seafood, and

208   egg analogs. Consequently, it is important to know and control these attributes.

209   *Interfacial properties*: The interfacial properties of the particles in NG-PB foods may also

210   impact their rheological properties, mainly because they influence the colloidal interactions

211   between them, which determines their aggregation state. Some of the most important interfacial

212   properties are their polarity, charge, and thickness [34]. Some particles found in NG-PB foods are

213   predominantly polar because they have a preponderance of hydrophilic groups on their surfaces,

214   including oil bodies, oil droplets, and plant-tissue fragments. Other particles are predominantly

215   non-polar because they have numerous hydrophobic groups on their surfaces, including protein

216   assemblies formed by zein or gliadin [35]. It should be noted that the polarity of particles may

217   change depending on the processing conditions used. For instance, the surfaces of oil droplets

218   coated with globular proteins may go from polar to non-polar when they are heated because the

219   adsorbed proteins unfold and expose hydrophobic groups [36].

220   The electrical characteristics of the particles in NG-PB foods are also important because they

221   influence their interactions with each other, as well as with other charged substances in the

222   system. Under neutral pH conditions, most kinds of particles found in NG-PB foods are

223   negatively charged or neutral. However, the charge on particles containing appreciable amounts

224   of proteins on their surfaces, such as oil bodies, oil droplets, or protein aggregates, may go from
225   negative to positive as the pH is reduced from above to below their isoelectric point [37-39]. This is
226   because the amino and carboxyl groups on the proteins become progressively protonated as the
227   pH is reduced ($-NH_2 \rightarrow -NH_3^+$ and $-COO^- \rightarrow -COOH$), which leads to an increase in positive
228   charge and decrease in negative charge. At the isoelectric point of the proteins, the number of
229   negative and positive charges are balanced, leading to a zero net charge. A reduction in the net
230   charge on the particles in a NG-PB food can promote their aggregation, which usually leads to an
231   increase in viscosity or gel strength [40, 41]. The controlled aggregation of proteins and protein-
232   coated oil droplets is important for the creation of NG-PB cheeses, which often rely on
233   isoelectric precipitation to form semi-solid structures.

234   For particles that are coated by polymeric materials, like proteins or polysaccharides, their
235   resistance to aggregation also depends on the thickness of the adsorbed layer [42]. Typically, the
236   strength of the steric repulsion between particles increases as the thickness of the adsorbed
237   polymer layer increases. Consequently, it may be important to control the thickness of an
238   adsorbed layer to manipulate the stability and rheology of these colloidal dispersions.

239

240   **Table 1:** Examples of the variations in the characteristics of particulate matter found in NG-
241   PB foods. The charge is given under neutral conditions. Under acidic conditions, proteins may
242   become positively charged (as in dressings or soft drinks). Key: TVP = texturized vegetable
243   protein.

244

Type	Composition	Diameter	Shape	Charge	Polarity
Oil bodies	Fat, protein, and phospholipids	100 to 5000 nm	Spherical	Negative	Polar coating
Oil droplets	Fat and emulsifier	100 to 5000 nm	Spherical	Negative	Polar coating
Colloidal protein	Protein	100 to 5000 nm	Spheroid	Negative	Polar to non-polar*
Protein fibrils	Proteins	Several nm	Fibrous	Negative	Polar to non-polar*
Starch granules	Starch	2 to 40 μm	Spheroid	Negative to neutral	Polar exterior
Plant tissue fragments	Dietary fiber	100 nm to 100 μm		Negative	Polar exterior

TVP	Protein	2 to 30 mm	Irregular chunks	Negative	Polar to non-polar exterior*

245   * The polarity of protein particles depends on the type used. Zein and gliadin are non-polar,

246   whereas most other plant proteins are polar (at room temperature).

247

248   In summary, when considering the rheological properties of a NG-PB food containing

249   colloidal particles it is important to have knowledge of their composition, size, shape, and

250   interfacial properties. This usually depends on having a range of suitable analytical tools to

251   provide information about these properties [1].

252   **3.2. Polymers**

253   The most important polymers in NG-PB foods are usually proteins and polysaccharides from

254   plant (or sometimes microbial) sources [1, 16]. These biopolymers vary in the number, type, and

255   sequence of monomers present, as well as the nature of the bonds between them. Proteins are

256   assembled from amino acids held together by peptide bonds, whereas polysaccharides are

257   assembled from monosaccharides held together by glycosidic bonds. In this section, we

258   highlight some of the most important attributes of the polymers present in NG-PB foods that may

259   influence their rheological properties.

260   *Composition*: The monomers that make up plant proteins and polysaccharides vary

261   considerably depending on their origin, which has a major impact on their physicochemical,

262   functional, and nutritional properties. For instance, the type of monomers present influences the

263   polarity and electrical characteristics of proteins and polysaccharides, which influences their

264   conformation, interactions, and ability to form gels. For proteins, the amino acid composition

265   also influences their nutritional attributes, such as the fraction of essential and non-essential

266   amino acids present, as well as their digestibility and bioavailability. For polysaccharides, the

267   type and bonding of monosaccharides influences their digestibility within the gastrointestinal

268   tract, which impacts their health benefits. For this reason, there is interest in utilizing dietary

269   fibers to create structures in NG-PB foods, rather than rapidly digestible starches. Consequently,

270   it is often important to establish the nature of the polymers used to formulate NG-PB foods, and

271   their impact on the texture.

272   *Molecular characteristics*: The molecular characteristics of polymers determine their impact

273   on the physicochemical, functional, sensory, and nutritional properties of NG-PB foods. Several

11

274   molecular characteristics are especially important, including the molecular weight, conformation,

275   branching, flexibility, polarity, and charge of the polymer chains [43, 44]. For instance, the ability

276   of polymers to thicken solutions or form gels is often influenced by their molecular weight [45].

277   Larger polymers are typically more effective at thickening and gelling than smaller ones. The

278   polarity and charge of polymers influences their interactions with other molecules [46, 47]. For

279   instance, the number of non-polar, polar, and charged groups impacts the hydrophobic, hydrogen

280   bonding, and electrostatic interactions between the polymer chains, which influences their

281   structuring and gelling properties. In turn, this influences the methods that can be utilized to

282   form gels from different kinds of polymers. As an example, polymers that can form strong

283   hydrogen bonds with each other (such as agar) can be gelled by cooling them to a temperature

284   where the polymer chains adopt helical structures that crosslink with each other through

285   hydrogen bonding. Polymers with a strong negative charge (like alginate, carrageenan, or

286   pectin) can be gelled by adding appropriate cations (like calcium or potassium) to form

287   electrostatic bridges. Polymers with a high surface hydrophobicity (like globular proteins above

288   their thermal denaturation temperature) can be gelled by heating them to promote their unfolding

289   and aggregation through hydrophobic attraction. Consequently, knowledge of the molecular

290   characteristics of the polymers used to formulate NG-PB foods is important for understanding

291   and controlling their formation and rheological properties.

4. Modelling of Rheological Properties of Fluid-like Plant-based Foods

293   Many NG-PB foods exhibit predominantly fluid-like characteristics, including milk, cream,

294   and fluid egg analogs. These systems are basically colloidal dispersions containing particles (like

295   oil bodies or fat droplets) and polymers (like hydrocolloids) dispersed in water (**Figure 1**).

296   Consequently, the theoretical models used to relate the rheological properties of these colloidal

297   dispersions to their composition and structure can be utilized to understand, predict, and control

298   the properties of fluid-like plant-based foods.

4.1. Types of fluid-like behavior

300   In general, fluids can be described as either ideal or non-ideal depending on how their

301   rheology changes with applied shear stress.

4.1.1. Ideal fluid behavior

303   The rheological properties of ideal fluids are described by their shear viscosity (η), which is

304   the slope of the shear stress *versus* shear rate. For this type of fluid, the shear stress (τ) is

305   directly proportional to the shear rate ($\dot{\gamma}$) and so their rheology can be described by the following

306   simple expression:

307

308          $$\tau = \eta\dot{\gamma} \tag{1}$$

309

310   The units of the shear stress are Pascals (Pa), whereas those of the shear rate are reciprocal

311   seconds (s^{-1}), and so the units of the apparent shear viscosity are Pa s. For ideal fluids, the shear

312   viscosity is independent of the applied shear rate.

313   *4.1.2. Non-ideal fluid behavior*

314   Several NG-PB foods exhibit non-ideal fluid behavior, which means the applied shear stress

315   is no longer proportional to the shear rate. The most common type of non-ideal behavior

316   observed in these products is shear-thinning, which refers to a decrease in shear viscosity with

317   increasing shear rate (or stress). For instance, the apparent shear viscosity of some milk or fluid

318   egg analogs decreases with increasing shear rate because they contain particles or polymers held

319   together by weak forces, which are disrupted when the applied shear stress is raised. In

320   principle, the apparent shear viscosity can also increase as the applied shear rate is raised, which

321   is known to as shear thickening, but this kind of behavior is less common in foods. One potential

322   cause of shear thickening is a greater tendency for polymers or particles to aggregate with each

323   other when the shear rate is raised because this increases the collision frequency between them.

324   The change in the apparent viscosity of non-ideal fluids with shear rate can be modeled using

325   the Cross model [48]:

326          $$\eta = \eta_\infty + \frac{\eta_0 - \eta_\infty}{1 + (K\dot{\gamma})^{1-n}} \tag{2}$$

327   In this equation, η_0 is the plateau apparent shear viscosity at very low shear rates, η_∞ is the

328   plateau apparent shear viscosity at very high shear rates, K is the Cross constant, and n is the

329   power index. The value of the power index provides information about the kind of non-ideal

330   behavior exhibited by the fluid: $n = 1$ for an ideal fluid; $n < 1$ for a shear thinning fluid; and $n > 1$

331   for a shear thickening fluid. The rheological behavior of this kind of non-ideal fluid can

332   therefore be described by finding the η_0, η_∞, K, and n parameters that give the best fit between

333   the model and experimental measurements of apparent shear viscosity *versus* shear rate. In

334   colloidal dispersions containing aggregated polymers or particles, the magnitude of K is

335   governed by the strength of the bonds holding the structures together [49]. An example of the

336   dependence of the apparent viscosity on shear rate predicted by the Cross model is shown in
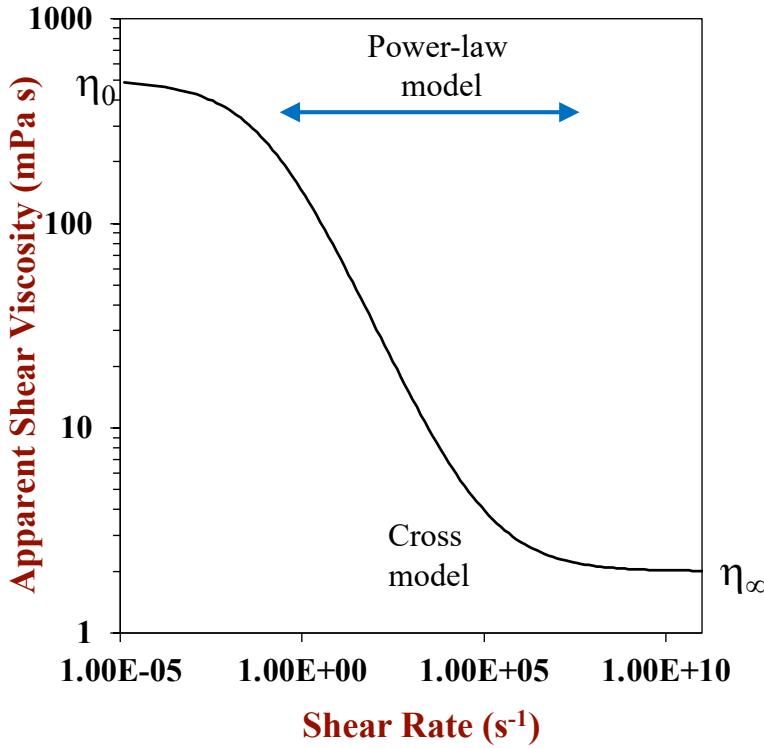
337   **Figure 3** for a shear thinning fluid.

339 **Figure 3.** The change in viscosity of non-ideal fluid NG-PB foods can often be described by the
340 Cross model. The power-law model is only applicable in the region where log(viscosity) is
341 proportional to log(shear rate).

343   In practice, it may only be possible to measure the apparent shear viscosity over intermediate

344   shear rates rather than the entire shear rate range, which extends many orders of magnitudes, due

345   to the limitation of existing rheometers. In this case, the apparent shear viscosity can sometimes

346   be described using a simple power law model [50]:

347    $\eta = K(\dot{\gamma})^{n-1}$ (3)

348   Here, K is the consistency index and n is the power index. In this situation, the rheology of a

349   fluid can be described by finding the K and n values that give the best fit between the model and

350   experimental measurements of apparent shear viscosity *versus* shear rate.

351   In some cases, the viscosity of non-ideal fluids depends on how long the shear stress is

352   applied to the sample. For example, the apparent shear viscosity may decrease (shear thinning)

353   or increase (shear thickening) over time depending on the nature of the sample. This kind of

354   shear thinning behavior may occur because structures within a sample (such as aggregated

355   polymers or particles) become increasingly disrupted the longer the shear stress is applied.

356   Conversely, this kind of shear thickening may occur if the applied shear stress induces particle or

357   polymer aggregation during the measurement.

358   **4.2. Theoretical models relating the rheology of colloidal fluids to their properties**

359   The theoretical models developed to describe the rheology of colloidal fluids are usually

360   based on calculations of the frictional losses that occur when a fluid flows around the particles or

361   polymers dispersed in a liquid during the application of a stress. Many fluid NG-PB foods can

362   be considered to be colloidal suspensions consisting of polymers or particles (like

363   polysaccharides, protein aggregates, oil bodies, oil droplets, or plant cell fragments) dispersed in

364   an aqueous solution. Their rheological properties can therefore be related to their composition

365   and structure using theoretical models developed to describe colloidal dispersions [48, 51]. In

366   general, the viscosity of a colloidal suspension increases as the concentration of polymers or

367   particles it contains is raised, with the magnitude of the rise being governed by the types of

368   polymers or particles present.

369   For dilute colloidal suspensions containing non-interacting rigid spherical particles, the shear

370   viscosity (η) can be related to the disperse phase volume fraction (ϕ) of the particles using an

371   equation first derived by Albert Einstein:

372        $\eta = \eta_1(1 + 2.5\phi)$ (4)

373   Here, η_1 is the shear viscosity of the aqueous phase surrounding the particles. This equation can

374   usually be employed when the disperse phase volume fraction is below around 0.05 (5%),

375   providing that other assumptions are met, *i.e.,* the particles are hard, rigid, and separate. When

376   the concentration of particles within a colloidal suspension increases the fluid flow around one

377   particle influences that around the neighboring particles, thereby leading to increased energy

378   dissipation. As a result, there is an increase in the viscosity over that predicted by the Einstein

379   equation. The viscosity of more concentrated colloidal suspensions can be modeled using a

380   semi-empirical equation derived using effective medium theory [48, 51]:

381        $\eta = \eta_1 \left(1 - \frac{\phi}{\phi_C}\right)^{-2}$ (5)

382   Here, ϕ_c is a critical packing parameter (≈ 0.65), which is assumed to be the volume fraction

383   where the colloidal particles become jammed together, leading to elastic-like properties.
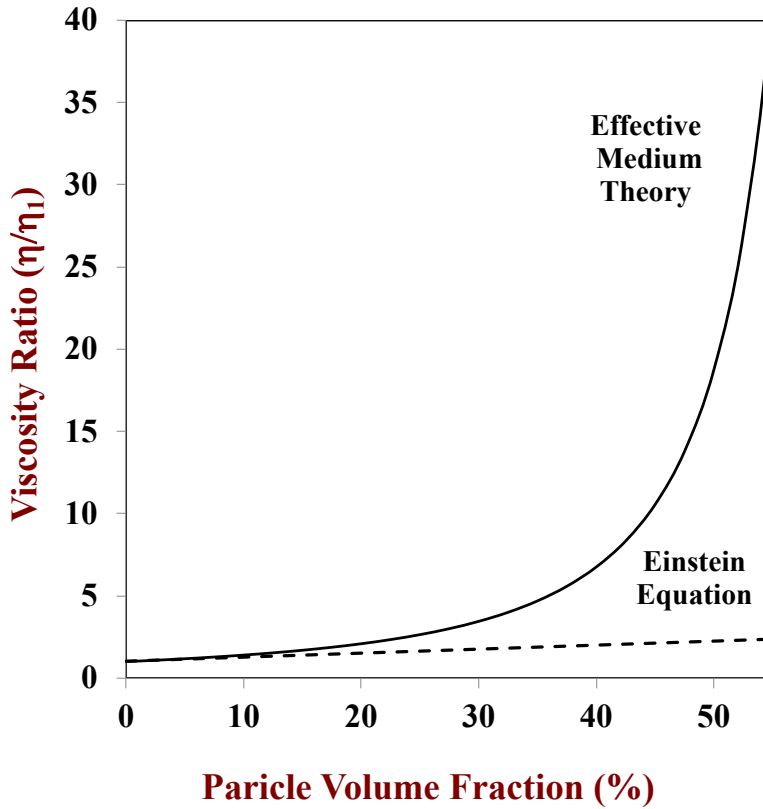
384

385

386   **Figure 4.** The increase in shear viscosity with increasing particle concentration for colloidal

387   particle dispersions can be described by the Einstein equation for dilute systems and by the

388   effective medium theory for concentrated systems

389

390   The increase in viscosity with increasing particle volume fraction predicted by these two

391   equations is plotted in **Figure 4.** At low volume fractions (< 5%), both equations give fairly

392   similar values, but at higher volume fractions the effective medium theory predicts a much

393   higher viscosity than the Einstein equation. The effective medium theory predicts that the

394   viscosity should increase steeply when the particle volume fraction exceeds about 45%, which is

395   because the particles start to strongly interact with each other. The impact of particle

396   concentration on the viscosity of colloidal suspensions is the reason why milk ($\phi < 5\%$ fat) has a

397   low viscosity, heavy cream ($\phi \approx 40\%$ fat) has a high viscosity, and mayonnaise ($\phi \approx 70\%$ fat) is a

398   semi-solid material.

399   Similar equations can be used to describe the rheological properties of colloidal suspensions

400   containing polymers. However, in this case the volume fraction of the particles (ϕ) should be

401   replaced by the effective volume fraction of the polymers (ϕ_{eff}):

402        $\phi_{eff} = R_V \phi$ (6)

403   Here, R_V is the volume ratio of the polymer molecules, which is the total volume occupied by

404   an individual polymer molecule in solution (polymer chain plus entrained water) divided by the

405   volume occupied by the polymer chain alone: $R_V = V_T/V_P$. This equation assumes that a polymer

406   molecule can be assumed to act like an effective sphere that perturbs the fluid flow within the

407   colloidal suspension. In this case, the effective sphere contains both polymer molecules and

408   solvent. The volume ratio of a polymer can be related to its molecular characteristics using the

409   following approximate equation:

410        $$R_V = \frac{4\pi r_H^3 \rho N_A}{3M}$$ (7)

411   Here, r_H is the hydrodynamic radius of the polymer molecules, ρ is the density of the polymer

412   chain, N_A is Avogadro's number, and M is the molecular weight of the polymer. Taken together,

413   these expressions indicate that the viscosity of a polymer solution should rise as the polymer

414   concentration is raised and the hydrodynamic radius of the polymer is increased (for a fixed

415   molecular weight). Thus, polymers with open extended structures (high r_H) should be more

416   effective thickening agents than ones with tight compact structures (low r_H). This explains why

417   polysaccharides like xanthan or gellan gum are highly effective at increasing the viscosity of a

418   solution, whereas globular proteins like soy or pea protein are not. For polymers of the same

419   conformation (*e.g.,* random coil), the volume ratio, and therefore viscosity, increases with

420   increasing molecular weight (even though M is in the denominator of the equation). This

421   phenomenon is a result of the fact that r_H and M are dependent variables, with the radius of

422   hydration increasing as the molecular weight increases. The relationship between the

423   hydrodynamic radius and molecular weight of polymers depends on their conformation: $r_H \propto M$

424   for rigid rods: $r_H \propto M^{1/2}$ for random coils; and $r_H \propto M^{1/3}$ for globular structures. Thus, R_V is

425   proportional to M^2, $M^{3/2}$, and M for rods, coils, and globules, respectively [52].
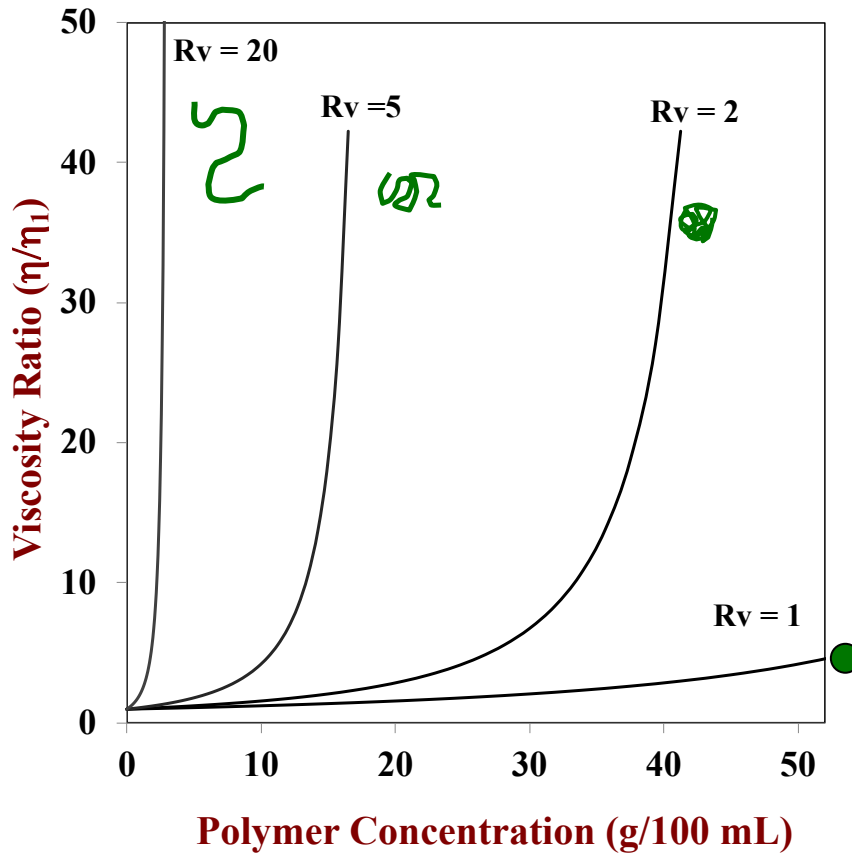
426

Figure 5. The increase in shear viscosity with increasing polymer concentration for polymer solutions depends strongly on the conformation of the polymers.

The predicted concentration-dependence of the viscosity of polymer solutions with different R_V values is shown in **Figure 5**. These predictions suggest that adding globular proteins ($R_V \approx$ 1) to an aqueous solution will only cause a pronounced rise in viscosity when the concentration exceeds about 30-40 g/100 mL. In contrast, adding polysaccharides with highly extended structures ($R_V \gg 1$) to aqueous solutions results in a pronounced rise in viscosity when the concentration exceeds a much lower value (< 1 g/100 mL). Knowledge of this effect is useful when selecting plant-based ingredients for application in some types of NG-PB food products. For instance, it may be important that a milk analog contains a high amount of protein but that it also has a low viscosity. In this case, it would be advantageous to select a protein source that has a compact globular structure, such as soy or pea protein. In contrast, a PB dressing product may need to be highly viscous to inhibit gravitational separation and to provide desirable textural attributes. However, it may be important that the ingredient costs and calorie content are not too

443 high. In this case, the viscosity of the product can be increased by adding a relatively low

444 concentration of a polysaccharide with a highly extended structure, such as xanthan, locust bean,

445 or gellan gum.

446 **4.3. Major factors impacting the rheology of colloidal fluids**

447 The theoretical models discussed in the previous section provide some important insights into

448 the major factors impacting the rheological properties of colloidal fluids containing polymers or

449 particles. Some of the most important factors are highlighted below:

450 *Continuous phase rheology*: The theoretical equations derived to describe the rheology of

451 colloidal fluids show that their viscosity is proportional to the viscosity of the continuous phase.

452 Consequently, increasing the viscosity of the continuous phase by adding thickening agents will

453 increase the overall viscosity of the system.

454 *Particle or polymer concentration*: The theoretical equations show that increasing the

455 concentration of the particles or polymers in a colloidal fluid increases the overall viscosity.

456 Typically, the viscosity increases relatively slowly with increasing concentration for dilute

457 systems, but then increases steeply when particle-particle or polymer-polymer interactions

458 become more important (**Figure 4**). Consequently, a critical concentration has to be exceeded

459 before the viscosity increases dramatically.

460 *Polymer conformation*: For polymers, their ability to increase the viscosity of a colloidal fluid

461 depends on their conformation. The greater the effective volume they occupy in solution (higher

462 R_V), the greater their thickening power (**Figure 5**). Consequently, larger stiffer linear polymers

463 tend to be the most effective at increasing the viscosity of colloidal dispersions, like xanthan

464 gum.

465 *Aggregation state*: The viscosity of colloidal fluids tends to increase when the particles or

466 polymers are aggregated because there is then an increase in the effective volume fraction

467 occupied by them. In other words, the disturbance in the fluid flow profile is greater, which leads

468 to greater energy dissipation due to friction, leading to a higher viscosity.

469 *Particle size*: Particle size does not have a major direct impact on the viscosity of colloidal

470 dispersions, as seen in the Einstein and effective medium theory equations shown earlier.

471 However, it may have an indirect effect by affecting the aggregation state and interactions

472 between the particles.

473 In general, the rheological properties of fluid foods can therefore be altered by changing the

474   type, concentration, and interactions of the polymers or particles they contain.

4.4. Examples of rheological properties of fluid NG-PB foods

476   In this section, several examples of the rheological behavior of fluid NG-PB foods, such as

477   plant-based milk or egg analogs is given. The shear viscosity, consistency index, and flow index

478   (determined from the power-law model) of selected NG-PB foods are summarized in **Table 3**.

479   At a constant shear rate (10 s^{-1}), the shear viscosity of these foods varies widely, from relatively

480   low for milk analogs to relatively high for plant-based salad dressings. The flow index of several

481   of the milk analogs is close to one ($n \approx 1$), which means they behave like ideal liquids, where the

482   shear viscosity does not depend strongly on shear rate. This is probably because they are

483   relatively dilute colloidal dispersions that contain particles or polymers that are not strongly

484   aggregated with each other. Several of the more viscous products, especially the dressings, have

485   flow indices much lower than unity ($n \ll 1$), which indicates that they are highly shear thinning

486   fluids. The pronounced decrease in the viscosity of these products with increasing shear rate can

487   be attributed to the presence of aggregated or entangled polymers or particles, like

488   polysaccharides, protein aggregates, oil bodies, oil droplets, or plant-tissue tissue fragments. As

489   the shear rate increases, the structures in these fluids become aligned, deformed, or disrupted,

490   thereby leading to a decrease in viscosity. The rheology of NG-PB foods that are highly

491   concentrated or contain aggregated polymers or particles, like some plant-based salad dressings

492   and mayonnaises, can be treated as plastic materials, which behave like a solid below a critical

493   yield stress but a fluid above this value. The equations used to describe these kinds of semi-solid

494   foods are discussed in section 5.1.2.

495

496   **Table 3.** Shear viscosities and rheological parameters of some NG-PB foods and animal-

497   based ones whose properties have been modeled by the power-law theory. Modified from

498   McClements and Grossmann [1].

Product type	Viscosity at 10 s^{-1} (mPa·s)	Consistency index K (Pa sⁿ)	Flow index (n)	Reference
Cow's milk	2.2-2.6	-	1.00	[8]
Almond milk	4.6-26.3	-	0.82-0.56	[8]
Oat milk	6.8	-	0.89	[8]
Soy milk	2.6-7.6	-	1.00-0.90	[8]
Hen's whole egg	28	-	1.00	[53]

Hens' egg white	26	0.140	0.33	54
NG-PB egg white	16	0.089	0.28	54
NG-PB whole egg	8.2			
Salad dressing	2400	15	0.21	55

499

5. Modelling of Rheological Properties of Solid-like Plant-based Foods

Several kinds of NG-PB foods exhibit predominantly solid-like properties, including meat, seafood, cooked egg, and cheese analogs (**Figure 6**). Nevertheless, they also exhibit some fluid-like properties, like viscoelasticity or plasticity, which means they should more strictly be considered to be soft solids. The rheology of colloidal soft solids is strongly influenced by the type, concentration, and interactions of the polymers and/or particles they contain. The elastic properties of many conventional animal sourced products are a result of the presence of a three-dimensional network of crosslinked polymers (commonly proteins). For instance, the solidity of meat and seafood products is a result of the complex hierarchical structures formed by various proteins (such as actin, myosin, and collagen) in the muscle and connective tissues, the solidity of cheeses and yogurts is a result of networks formed by aggregated casein molecules, whereas the solidity of cooked eggs is a result of networks of aggregated globular proteins from egg white and egg yolk. NG-PB foods designed to mimic the textural attributes of animal sourced foods therefore often use food polymers, like proteins, starches, and/or gums, to create network structures that provide similar textural attributes to the animal-based products they are designed to replace [2].
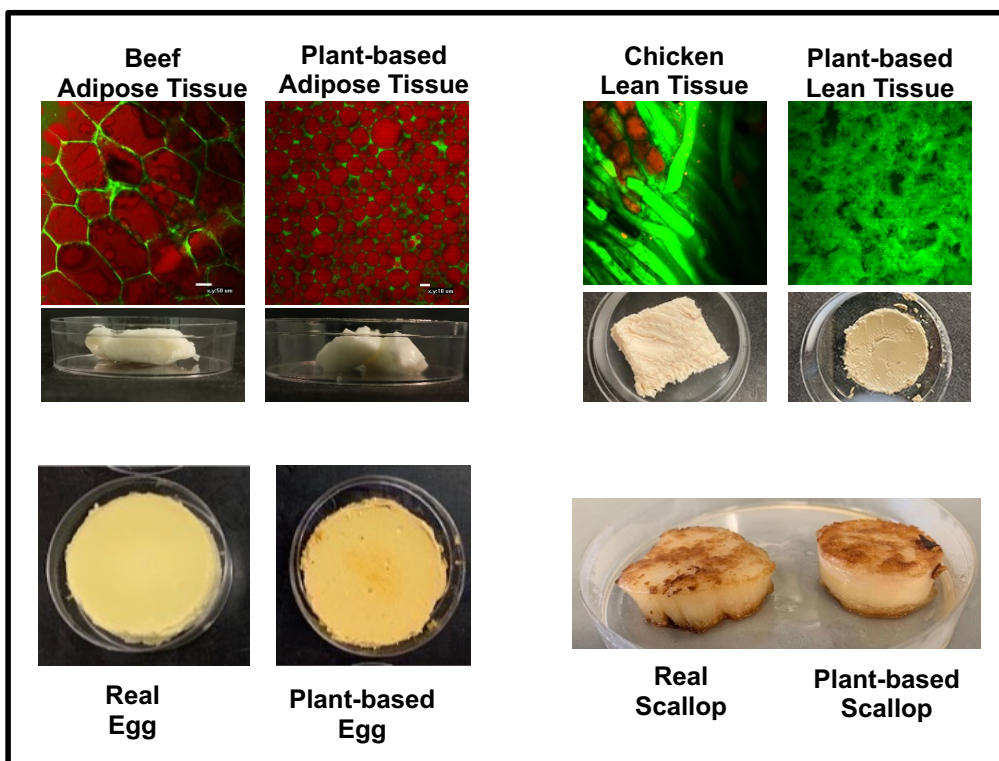
Figure 6. Examples of solid-like plant-based analogs of animal sourced foods like meat, seafood, and eggs. These products were all prepared in the authors laboratory from plant-based proteins, polysaccharides, and lipids.

It should be noted, however, that there are other components in animal sourced foods that also impact their overall textural attributes, including adipose cells in meat and seafood, milk fat globules in dairy products, lipoproteins in egg yolk, ice crystals and air bubbles in ice cream, and fat crystals in cheese and butter. As a result, food formulators often employ analogous plant-based ingredients to simulate the textural attributes normally provided by these structural elements in NG-PB foods, including oil droplets, air bubbles, and fat crystals.

The rheology of soft solids is also dependent on the type of non-covalent and/or covalent bonds acting between the various structural elements they contain, such as van der Waals, hydrogen bonding, hydrophobic, electrostatic, and chemical interactions [48]. The sign (attractive or repulsive), magnitude (weak to strong), and range (short to long) of non-covalent interactions is often influenced by solution and environmental conditions, such as pH, ionic strength, and temperature. As a result, the rheological properties of solid-like NG-PB foods can be manipulated by controlling these parameters during their manufacturing and preparation.

534 Covalent bonds are typically stronger and more robust than non-covalent ones. They may be

535 established between the structural elements within a NG-PB food through chemical reactions,

536 such as the Maillard reaction or disulfide bond formation, or through enzymatic crosslinking

537 reactions, such as those promoted by transglutaminase or laccase. The textural attributes of these

538 foods can therefore be manipulated by controlling the reaction conditions to alter the type and

539 number of crosslinks formed between the structural elements in a NG-PB food, such as proteins

540 and polysaccharides. It is therefore important to understand the chemical reactivity of the

541 different structural elements in these foods, so that solution and environmental conditions can be

542 altered to induce the network formation required for specific applications.

543   In general, the textural attributes of solid and semi-solid foods are often characterized in terms

544 of their elastic modulus and fracture properties [56]. The elastic modulus provides an indication of

545 the ability of the material to resist deformation when a force is applied: the higher the elastic

546 modulus, the harder the material. The fracture properties provide an indication of the ability of a

547 material to resist rupture when a force is applied. They can be represented by the minimum

548 stress needed to promote disruption (fracture stress), as well as the relative change in the

549 dimensions of the material before it first becomes disrupted (fracture strain). These parameters

550 are related to the brittleness and malleability of materials (Section 5.1.2). Several kinds of NG-

551 PB foods exhibit plastic-like behavior, where they act as a solid below a critical yield stress, but

552 a fluid above this value, including PB meat, seafood, cheese, yogurt, and spreads. It is important

553 to control the rheology of these foods because they impact their physicochemical, functional, and

554 sensory properties, such as hardness, softness, brittleness, malleability, spoonability,

555 spreadability, cutting, and eating attributes. Even though solid-like NG-PB foods display a wide

556 variety of textural attributes, their rheology can often be characterized using only a small number

557 of mathematical models [57]. Some of these models are simply descriptive models developed to

558 describe the rheological properties of a material in terms of a few key parameters, whereas others

559 are based on a mathematical analysis of the physics of colloidal suspensions containing

560 interacting polymers or particles. These models can be used to relate the composition, structure,

561 and interactions of colloidal suspensions to their rheological properties in a more rigorous

562 fashion and provide important information about the key parameters that influence their

563 rheology.

564 **5.1. Types of solid-like behavior**

23

565   Like fluids, the rheological properties of solid-like foods can be described as ideal or non-

566   ideal depending on how they respond to an applied stress.

567   *5.1.1. Ideal solid behavior*

568   The rheological properties of ideal solids are usually characterized by plotting the applied

569   stress (τ) *versus* the resulting strain (γ), with the slope of this line being equal to the elastic

570   modulus (E) of the material (**Figure 7**). This relationship is described by Hooke's law: $\tau = E \times \gamma$.

571   Methods for measuring the elastic modulus of solid-like materials using compression or shear

572   tests have been described elsewhere [1]. For compression tests, Youngs modulus (Y) is usually

573   used, whereas for shear tests, the shear modulus (G) is usually used.

574

575

576   **Figure 7.** The rheology of ideal solids can be described by their elastic modulus, while the

577   rheology of ideal plastics can be described by their yield stress and plastic viscosity.

578

579   In general, the mechanical properties of solid colloidal materials are governed by the types

580   and concentrations of particles and/or polymers they contain, as well as the number, orientation,

581   and strength of the forces acting between them [58]. Theories developed to describe their

582   properties are based on an analysis of the number of bonds present between the particles, as well

583   as the strength of each bond, which depends on the change in interaction potential with distance

584   (**Figure 8**).

STRESS

Bond strength

w(s)/kT

s (nm)

Particle Gel

Bond density
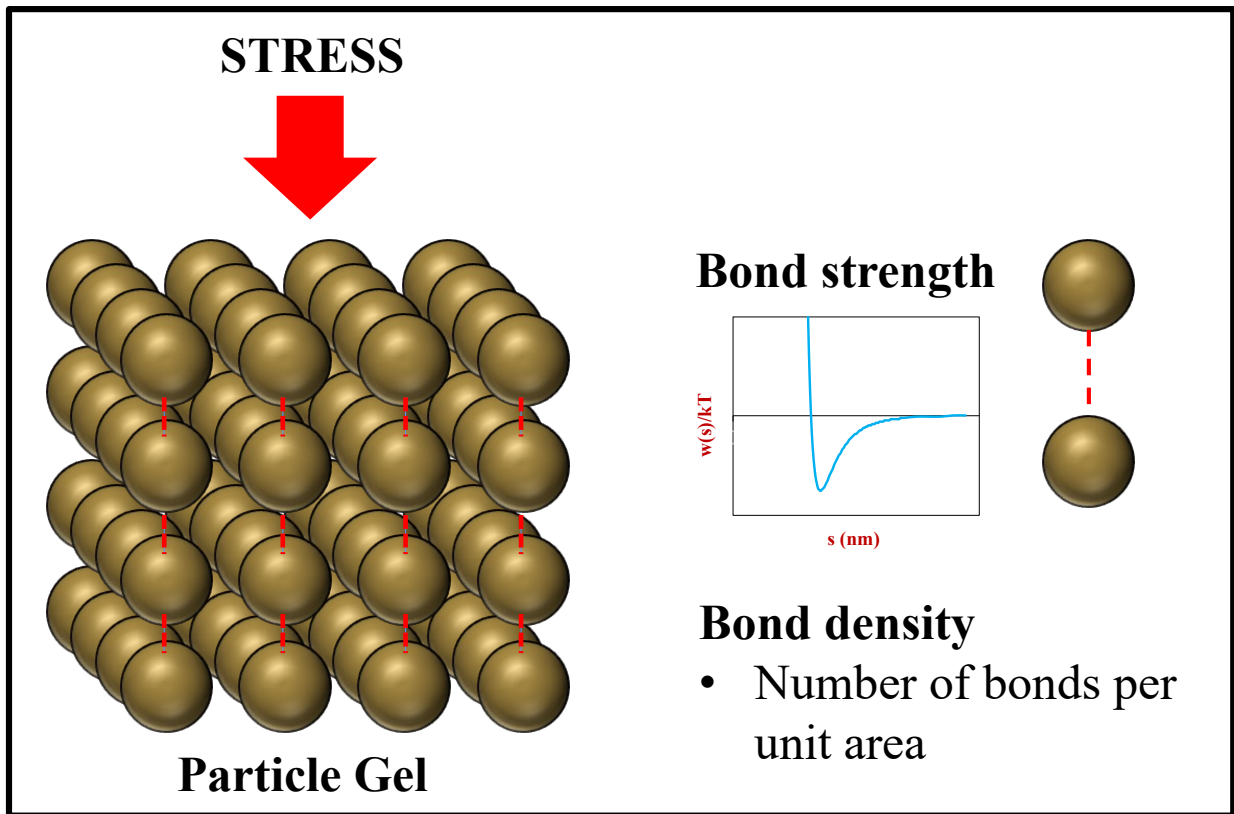- Number of bonds per unit area

585

586   **Figure 8.**   Highly schematic representation of a particle gel. The rheology of this type of gel
587   depends on the strength and density of the bonds between the different particles. The stronger
588   and more numerous the bonds, the greater the modulus.

589

590   Applying a stress to the surface of a colloidal solid causes the bonds between the structural

591   elements to become deformed, which causes the material to become compressed, with the extent

592   of compression depending on the number and strength of the bonds. For an ideal solid, all of the

593   energy applied to the material is stored within these bonds while the stress is applied but is

594   released when the stress is removed, and the material returns to its initial state. The elastic

595   modulus of a colloidal solid tends to increase as the number and strength of the bonds between

596   the structural elements rises. Researchers have developed several mathematical models to relate

597   the structure, composition, and interactions of colloidal solids to their rheological attributes.

598   These models are usually based on a theoretical analysis of the forces acting between the

599   particles or polymers in a colloidal material (see Section 5.2).

600   *5.1.2. Non-ideal solid behavior*

601 A linear relationship between stress and strain is typically only observed at low strains for

602 most solid or semi-solid NG-PB foods. At somewhat higher strains, this relationship becomes

603 non-linear, and at still higher strains, the material may become ruptured, and a break occurs in

604 the stress-strain curve. Moreover, many NG-PB foods exhibit both solid-like and liquid-like

605 behavior, either simultaneously (viscoelastic materials) or sequentially (plastic materials). More

606 sophisticated mathematical models are required to describe the rheology of these kinds of non-

607 ideal solids.

608 *Fracture properties*: At relatively low strains (< 1%), solid NG-PB foods often act as ideal

609 solids where the stress is linearly related to the strain. However, at higher strains they may

610 become temporarily or permanently disrupted because the bonds holding the different structural

611 elements together are broken. In some cases, the bonds may repair themselves once the stress is

612 removed (self-healing systems), whereas in other cases the bonds do not recover, and so the

613 fracture is permanent. Knowledge of the behavior of NG-PB foods at large strains is practically

614 important because it influences their resistance to mechanical forces during storage and

615 transport, as well as their behavior during food preparation (cutting, slicing, or spreading), and

616 consumption (chewing) [56, 58, 59].
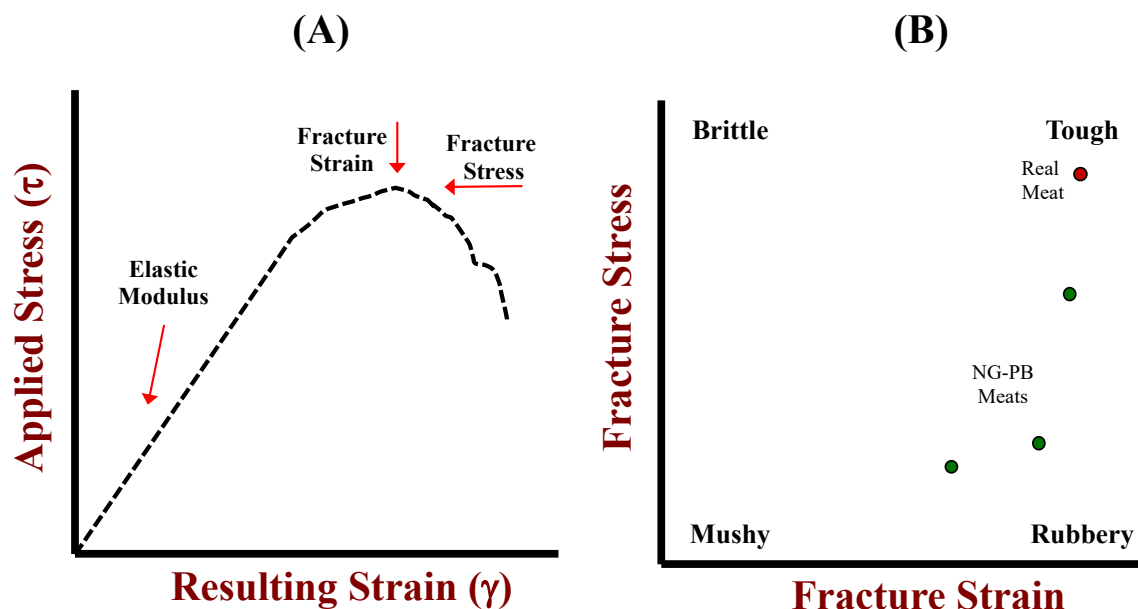

(A) **(B)**

617

618 **Figure 9.** **(A)** The fracture properties of solid or semi-solid NG-PB foods can be characterized by measuring the relative

619 deformation (strain) of the material as the magnitude of the applied force per unit area (stress) is increased. The elastic modulus,

620 fracture stress and fracture strain can be determined from this stress-strain profile. (B) A 2D Texture Map can be used to

621   characterize the fracture properties of NG-PB foods and compare them to real ones.

622

623   When the applied stress is no longer proportional to the resulting strain, an *apparent* elastic

624   modulus can be defined, which is equal to the slope of the stress *versus* strain plot at a particular

625   strain value. In this region, the food may still return back to its original shape once the applied

626   stress is removed. However, after a particular stress is exceeded, the food may flow or fracture

627   and so not return back. The *fracture stress* (τ_{Fr}) *and fracture strain* (γ_{Fr}) of a food can be

628   determined from a plot of the applied stress *versus* the resulting strain (**Figure 9**). These

629   parameters can then be represented on a 2-D map, which is useful for comparing the behavior of

630   NG-PB foods with the animal-based ones these are designed to replace. Foods that fracture at

631   low strains/low stresses are referred to as *mushy*, those that fracture at low strains/high stresses

632   are referred to as *brittle,* those that fracture at high strains/low stresses are referred to as *rubbery*,

633   and those that fracture at high strains/high stresses are referred to as *tough*. Foods tend to

634   fracture when the forces holding their structural elements together, such as proteins,

635   polysaccharides, or colloidal particles are exceeded [58]. Fracture often starts at locations within a

636   material where the bonds are relatively weak, such as cracks or dislocations. For this reason,

637   controlling the number and location of these discontinuities within a food may be important to

638   obtain the required fracture properties.

639   *Ideal plastics:* NG-PB foods like cream cheese, butter, and mayonnaise analogs have

640   rheological characteristics that can be described as plastic. These materials act like elastic solids

641   below a critical applied stress, known as the yield stress, but they act like liquids when the yield

642   stress is exceeded. When a shear stress is applied to an ideal plastic, its rheological properties

643   can be modelled using the following expressions:

644       $\tau = G\gamma$ when $\tau < \tau_Y$ (8)

645       $\tau - \tau_Y = \eta\dot{\gamma}$ when $\tau \geq \tau_Y$ (9)

646   Here, $G,\ \tau_Y$, and η are the shear modulus, yield stress, and plastic viscosity of the material.

647   Thus, the applied stress is proportional to the strain below the yield stress (like an ideal elastic

648   solid) but it is proportional to the rate of strain above the yield stress (like an ideal viscous

649   liquid). The stress-strain rate relationship for an ideal plastic material is shown in **Figure 7**.

650   When developing a NG-PB food that exhibits this kind of rheological behavior it is important to

651 match the elastic modulus, yield stress, and plastic viscosity to that of the animal sourced food it

652 is intended to substitute. The rheology of plastic materials is usually characterized by measuring

653 the stress *versus* strain or stress *versus* rate of strain profile using compression or shear testing

654 instruments [1].

655   At the structural level, NG-PB foods with plastic properties typically consist of 3D networks

656 of particles or polymers that interact with each other through relatively weak attractive forces.

657 For instance, cream cheese or yogurt analogs usually consist of a network of protein or

658 polysaccharide molecules dispersed in a liquid aqueous phase, whereas butter analogs consist of

659 a network of solid fat crystals dispersed in a liquid oil phase. When the stresses applied to this

660 kind of material are less than the yield stress, the bonds holding the particles or polymers

661 together within the 3D network are deformed but not disrupted. Once, the stresses are removed

662 the bonds give up the energy stored within them and return to their original shape, thereby

663 exhibiting elastic-like behavior. In contrast, when the applied stresses are greater than the yield

664 stress of the material, the bonds between the particles or polymers are disrupted and the material

665 starts to flow, which leads to liquid-like behavior. The ability of some foods to exhibit plastic

666 behavior is essential for their commercial applications. For instance, the spreadability of cream

667 cheese or butter analogs, the pourability of mayonnaise analogs, and the spoonability of yogurt

668 analogs all depend on these kinds of material properties. Examples of the rheological parameters

669 of selected NG-PB foods that can be considered to be non-ideal plastic materials are compared to

670 those of animal-sourced foods in **Table 4**.

671   **Table 4.** Examples of the rheological parameters of selected animal-sourced foods and NG-
672 PB foods that can be characterized as non-ideal plastics. Their rheological properties were
673 described by fitting the Herschel-Bulkley model to the shear stress *versus* shear strain curves.
674 Adopted from McClements and Grossmann [1].
675

	Yield Stress (Pa)	Consistency index K (Pa s^n)	Flow index (n)	Ref.
Dairy yogurt	11.7	2.50	0.55	[60]
Almond yogurt	28.4	6.45	0.37	[60]
Soy yogurt	27.2	3.52	0.45	[60]
Whole hen's egg	0.20	0.030	0.97	[53]
Whole NG-PB egg	9.7	0.11	0.95	Our laboratory

Salad dressing	47	16.3	0.52	[61]
Mayonnaise analog	81.4	82.6	0.21	Our laboratory

676

677   *Non-ideal plastics*: Many NG-PB foods have predominantly solid-like properties below a

678   critical yield stress but have liquid-like properties at higher stresses and can therefore be

679   considered to be plastic-like materials. However, they do not behave like ideal elastic materials

680   below the yield stress and/or ideal viscous materials above the yield stress, and so they can be

681   considered to be non-ideal plastics. As an example, these foods may undergo some flow when a

682   stress is applied below the yield stress, and they may exhibit shear thinning or shear thickening

683   behavior about the yield stress. For these kinds of material, it may be difficult to accurately

684   determine the yield stress because some flow occurs even at low applied stresses. This kind of

685   behavior may be exhibited by NG-PB foods whose structures are gradually disrupted over a

686   range of applied stresses, rather than due to an abrupt disruption of the structures at a specific

687   applied stress.

688   The rheological behavior of non-ideal plastics that behave like ideal solids below the yield

689   stress but like non-ideal liquids above the yield stress can be described by the Herschel-Bulkley

690   (HB) equation:

691     $\tau = \tau_Y + K\dot{\gamma}^n$ for $\tau \geq \tau_Y$ (10)

692   Here, *K* is the plastic consistency index and *n* is the plastic flow index. The values of these

693   parameters can be found by fitting the HB equation to the experimental data. Several

694   representative values of the τ_Y, *K* and *n* parameters obtained by fitting this model to experiments

695   on NG-PB food products or animal-source products are shown in **Table 4**. When designing NG-

696   PB foods it is usually desirable to ensure that their yield stress, consistency index, and flow index

697   match those of the animal sourced food they are intended to replace.

698   *Viscoelastic materials:* NG-PB foods such as meat, seafood, and egg analogs are viscoelastic

699   materials that exhibit both viscous- and elastic-like properties simultaneously [56, 58, 59]. When a

700   fixed shear stress is applied to an ideal viscous material it flows at a fixed shear rate as long as

701   the stress is applied. The shear rate increases linearly as the applied shear stress is increased,

702   with the slope being the shear viscosity. The viscous flow leads to energy dissipation due to

703   frictional losses. In contrast, when a fixed shear stress is applied to an ideal elastic material it

704   deforms to a fixed strain as long as the stress is applied, but then returns back to its original

705   shape when the stress is removed. The relative deformation (strain) of the material increases

706   linearly as the applied shear stress is increased, with the slope being the elastic modulus. In this

707   case, all of the energy that was originally stored in the bonds during compression, is released

708   during deformation, so the material returns back to its original shape and there is no energy

709   dissipation associated with frictional losses. When a stress is applied to a viscoelastic material it

710   behaves like both an elastic solid and a viscous fluid at the same time because it is both deforms

711   and flows. As a result, part of the energy is stored in the material and part of it is lost as heat due

712   to friction. Consequently, a *viscoelastic* material does not instantaneously deform to a new shape

713   when a stress is applied and does not instantaneously return to its original shape after the stress is

714   removed (**Figure 10**). Viscoelastic materials can be characterized as viscoelastic solids or

715   liquids depending on how they respond to an applied stress. When a stress is applied to a

716   viscoelastic solid it deforms at a finite rate (rather than instantaneously) until it reaches a fixed

717   deformation but once the stress is removed its dimensions return to their original values at a

718   finite rate. Many NG-PB meat, seafood, and cheese analogs exhibit this kind of behavior,

719   provided the stress is not too large to cause fracture. When a stress is applied to a viscoelastic

720   liquid it continues to flow as long as the stress is applied but when the stress is removed it only

721   partially recovers its original shape. NG-PB mayonnaise and cheese spreads exhibit this kind of

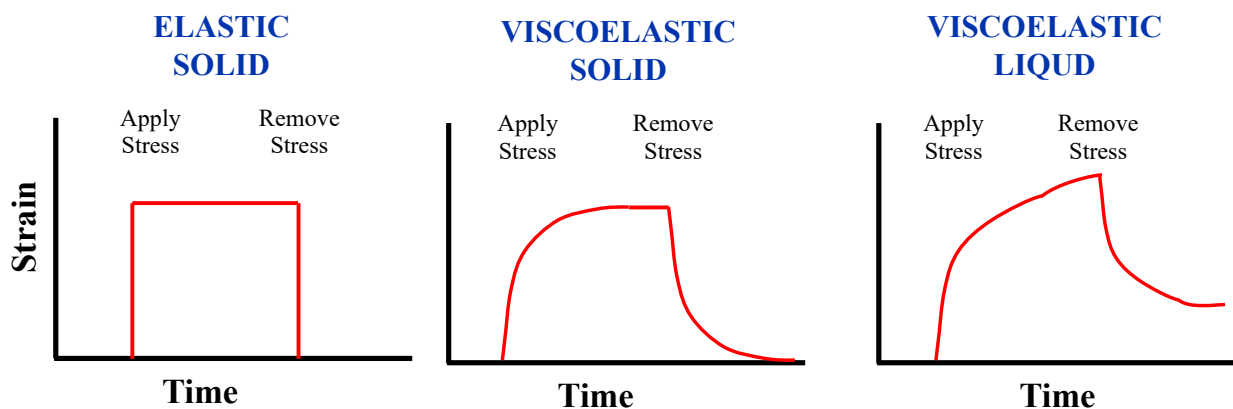722   behavior.

723

724   **Figure 10.**   Many solid or semi-solid NG-PB foods demonstrate viscoelastic behavior because
725   they act as solids and liquids simultaneously.

726

727   The rheology of viscoelastic materials is usually characterized by measuring their dynamic

728 shear rheology (*G*) as a function of time, frequency, strain, or temperature. A sample is placed in

729 the measurement cell of the rheometer and then an oscillating shear stress is applied and the

730 magnitude and phase of the resulting oscillating shear strain is measured [56, 59]. The storage (G')

731 and loss (G") modulus or the complex shear modulus (*G**) and phase angle (δ) are then plotted

732 *versus* the parameter of interest.

5.2. Theoretical models relating the rheology of colloidal solids to their properties

734 The most suitable theoretical model for describing the rheological properties of a particular

735 NG-PB food depends on the type of structural elements it contains, as well as their spatial

736 organization and interactions. An egg analog made from globular proteins (like soy, pea, or

737 mung bean protein) may be treated as a colloidal solid containing monodisperse spheres that

738 interact with each other. A cheese analog comprised of fat droplets embedded in a protein

739 network may be treated as a complex composite material containing spheres embedded in a

740 polymer matrix. A meat analog composed of phase separated protein-rich and polysaccharide-

741 rich regions organized into fibrous structures may be treated as an anisotropic two-phase

742 material. Consequently, it is important to identify the main structural elements in a NG-PB food,

743 and to establish their structural organization, when trying to identify a suitable theory to describe

744 their properties. Once an appropriate theoretical model has been identified then it can be used to

745 give useful insights into the main factors influencing the rheology of the material, such as

746 particle size, concentration, arrangement, or interaction strength [62]. In the remainder of this

747 section, mathematical models that have been developed to describe the rheology of different

748 kinds of solid colloidal dispersions that may be representative of NG-PB foods are considered.

749 *5.2.1. Polymer matrices*

750 Some types of NG-PB foods can be considered to be polymer matrices consisting of a

751 network of entangled or crosslinked polymer molecules. Consequently, theories developed to

752 describe the properties of polymer matrices can be utilized to understand, predict, and control

753 their behavior. For example, the following mathematical model has been derived to predict the

754 rheological properties of polymer materials containing a network of semi-flexible filaments [63]:

755 $$G \approx \frac{6\rho\kappa^2}{k_B T l_C^3} \qquad (11)$$

756 In this equation, *G* is the shear modulus, ρ is the filament length density, κ is the bending

757   rigidity of the filaments, l_C is the average distance between the crosslinks, k_B is Boltzmann's

758   constant, and T is the absolute temperature. Analysis of this equation provides some useful

759   insights into the importance of the major factors impacting the shear modulus of this kind of

760   polymer material. For instance, the equation predicts that the shear modulus increases as the

761   concentration of filaments rises (through ρ), as the stiffness of the filaments rises (through κ),

762   and as the crosslinking density of the filaments rises (through l_C). This model is based on an

763   analysis of the entropy and enthalpy effects occurring within the polymer network when it is

764   deformed. These effects depend on the number of configurations the filaments can adopt, as

765   well as their resistance to being deformed. This equation may be useful for modeling the

766   rheological properties of meat and seafood analogs containing fibrous networks of semi-flexible

767   polymers. Atomic force microscopy analysis has shown that gellan gum forms this kind of

768   polymer network [64], which is a commonly used ingredient in some plant-based foods.

769   *5.2.2. Particle gels*

770   Some NG-PB foods are formed by inducing the aggregation of globular proteins, such as

771   meat, seafood, and egg analogs [1]. In this case, it is often possible to use theoretical models

772   developed to describe the properties of colloidal particle gels consisting of a network of

773   aggregated spheres that extend throughout the volume of a system (**Figure 11**). Several

774   theoretical approaches have been utilized to develop relationships between the composition,

775   structure, and interactions of particle suspensions and the rheological properties of the gels they

776   form, which have been reviewed in detail elsewhere [51, 65, 66].
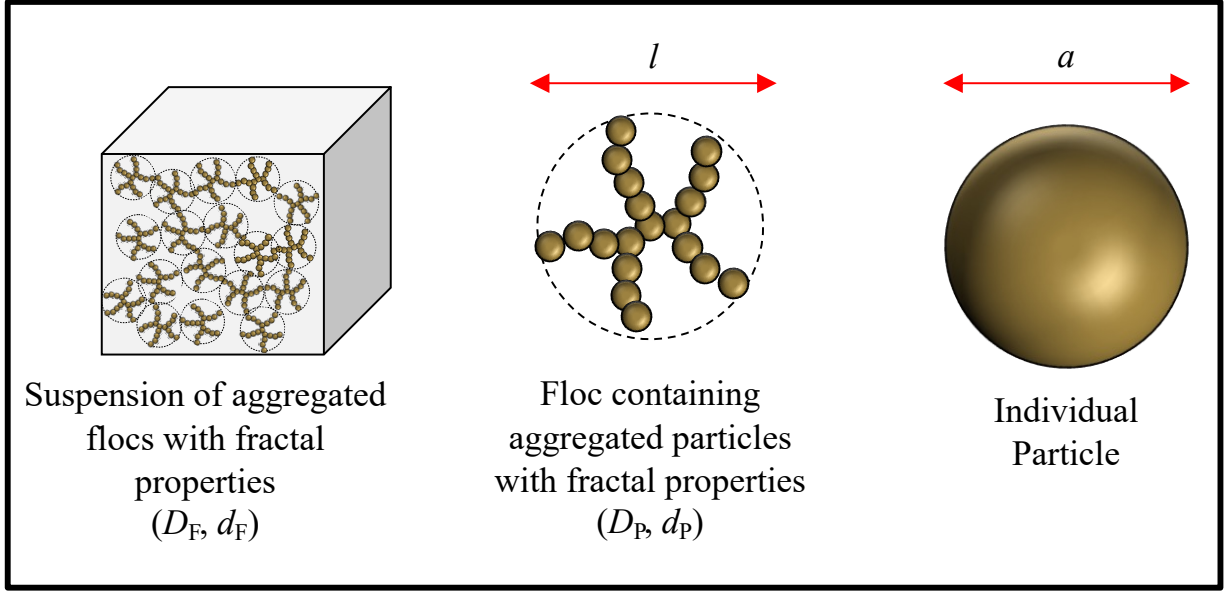
Figure 11. Many solid or semi-solid NG-PB foods can be considered to be particle gels, made up of networks of aggregated particles. These networks can have a fractal structure.

In this section, a theoretical model recently developed to describe the rheology of colloidal suspensions containing aggregated spherical particles assembled into fractal structures is considered [67]. This model assumes that the rheological properties of the colloidal suspensions can be related to their microstructure by assuming that the individual particles are assembled into flocs with a fractal structure, and that these flocs then aggregate with each other to form a network with another fractal structure (**Figure 11**). It also assumes that the bonds between the particles and flocs can be considered to act like springs that can bend or stretch. The elastic component (G') of the shear modulus can then be related to the composition, microstructure, and interactions of the system using the following expression:

$$G' = \frac{U}{a\delta^2} \phi^{\frac{2+f(d_F)}{3-D_F}} \left(\frac{l}{a}\right)^{\frac{3-D_P}{3-D_F}(2+f(d_F))-(2+f(d_P))} \tag{12}$$

Here, U is the interaction potential between a pair of aggregated particles, a is the diameter of the individual particles, δ is the distance between a pair of aggregated particles, ϕ is the volume fraction of the particles present in the overall system, l is the diameter of the flocs, D_P is the fractal dimension of the particles inside the flocs, d_P is the fractal dimension (from 1.1 to 1.4) of the elastic backbone inside the flocs (*i.e.,* the load bearing particles), D_F is the fractal dimension of the aggregated flocs in the overall system, and d_F is the fractal dimension (from 1.1 to 1.4) of

797 the elastic backbone of the aggregated flocs in the overall system (*i.e.,* the load bearing flocs).

798 The function in this equation, f(x), is related to the relative strength of the interactions between

799 the particles compared to the flocs, as well as to the degree of bending or stretching experienced

800 by the load bearing units [67]:

801   f(x) = α(2ε+x)-1   (13)

802   Here, α is a parameter that varies between 0 (weak-link regime) to 1 (strong-link regime), and

803 ε is a parameter that varies from 0 for pure stretching to 1 for pure bending. In the weak-link

804 regime, the overall rheological properties of the system are dominated by the strength of the

805 interactions between the individual particles inside the flocs, whereas in the strong-link regime

806 they are dominated by the strength of the interactions between the flocs. The fractal dimension

807 (D) of a system is determined by the nature of the interactions between the particles [66]. In

808 diffusion-limited cluster aggregation (DLA), the particles are strongly attracted to each other and

809 tend to stick to each other at the place they first make contact as they move around due to

810 Brownian motion, leading to a more open structure being formed. The fractal dimension of pure

811 DLA behavior has been estimated to be 1.78. In reaction-limited aggregation (RLA), the

812 particles are only weakly attracted to each other and so do not always stick together when they

813 first come into contact. Consequently, the particles in aggregates can undergo rearrangements

814 leading to more compact structures being formed. The fractal dimension of pure RLA behavior

815 has been estimated to be 1.99. In practice, other values can be obtained depending on the nature

816 of the aggregation mechanism with extreme values ranging from around 1 for a highly open

817 structure to around 3 for a highly compact structure.

818   The same theoretical approach has also been used to derive mathematical equations to

819 describe the plastic behavior of colloidal fractal gels [67]. These equations are typically based on

820 an analysis of the force required to disrupt the bonds between the structural elements in the gel [4].

821 The double fractal model has been used to relate the yield stress (τ_Y) and yield strain (γ_Y) to the

822 concentration, structural organization, and interactions of the spherical particles in a gel:

823     $$\gamma_Y = \frac{\delta}{a} \phi^{\frac{-f(d_F)}{3-D_F}} \left(\frac{l}{a}\right)^{-\frac{3-D_P}{3-D_F}f(d_F)+f(d_P)}$$ (14)

824

825
$$\tau_Y = \frac{U}{a\delta^2} \phi^{\frac{2}{3-D_F}} \left(\frac{l}{a}\right)^{\frac{2(D_F-D_P)}{3-D_F}}$$
(15)

826

827   The equations for G', γ_Y, and τ_Y can be simplified considerably if assumptions are made about

828   the nature of the system. For example, if it is assumed that the fractal properties of the particles

829   and flocs are similar ($D_F = D_P$, and $d_F = d_P$) and that particle-particle interactions dominate

830   (weak-link regime: $\alpha=0$), then these equations become:

831   $$G' = \frac{U}{a\delta^2} \phi^{\frac{1}{3-D_P}}$$
(16)

832   $$\gamma_Y = \frac{\delta}{a} \phi^{\frac{1}{3-D_P}}$$
(17)

833   $$\tau_Y = \frac{U}{a\delta^2} \phi^{\frac{2}{3-D_P}}$$
(18)

834   These equations suggest that the shear modulus and yield stress should increase as the strength of

835   the interactions between the particles increases, the particles become smaller, the distance

836   between the particles decreases, or the fractal dimension decreases. They also predict that the

837   yield strain should increase as the particle size or fractal dimension decrease, or as the distance

838   between the particles increases. This kind of knowledge can be used to design NG-PB foods

839   with enhanced rheological properties. For instance, the pH, ionic strength, or temperature may

840   be altered to increase the strength of the attractive forces between the individual proteins, which

841   will increase the interaction potential (U) and decrease the fractal dimension (D), thereby

842   increasing the overall strength of the protein gel. Alternatively, the size or concentration of

843   protein molecules used to formulate the gel can also be altered to modulate its properties.

844   The above equations will only be valid when the flocs form a network that occupies the entire

845   volume of the system, which will occur when the percolation threshold is exceeded. To a first

846   approximation, this concentration can be obtained from the following equation: $\phi_{eff} = \phi_F(l/a)^{3-D_F}$

847   $= 1$, where ϕ_{eff} and ϕ_F are the effective volume fraction and actual volume fraction of the flocs in

848   the system [67]. By accounting for the fact that the flocs are occupied by particles, a critical

849   particle volume fraction (ϕ_{crit}) for percolation can be obtained:

850   $$\phi_{crit} = (a/l)^{6-D_F-D_P}$$
(19)

851   This expression predicts that the volume fraction of particles required to form a 3D network

852   that extends throughout the system, and therefore gives elasticity, should decrease as the floc

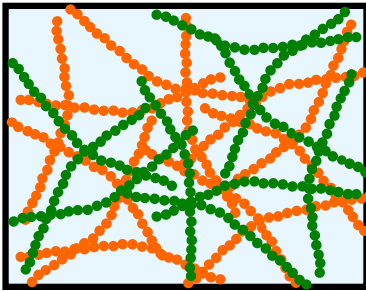853   dimensions increase (l) and the fractal dimensions (D_F and D_F) decrease.

854   Computer simulations have proven to be a powerful tool for understanding the microstructure

855   and rheological properties of colloidal particle gels [68]. These simulations show how the

856   structural organization and rheology of particle gels depend on the size, concentration, and

857   interactions of the particles they contain. This knowledge can then be used to guide the

858   ingredients and processing conditions used to create particle gels with the required properties.

859   It is important to note that the models used to describe the rheological properties of colloidal

860   particle gels are often too simplistic for understanding the properties of real protein gels. These

861   models often assume that the particles are homogeneous spheres, whereas protein ingredients

862   often contain a mixture of different proteins that have different sizes, shapes, and heterogeneous

863   surface chemistries, which alters the nature of the structures formed when they aggregate. For

864   instance, they may have hydrophobic patches at some locations on their surfaces, which limit the

865   places where they can form bonds with their neighbors, thereby altering their structural

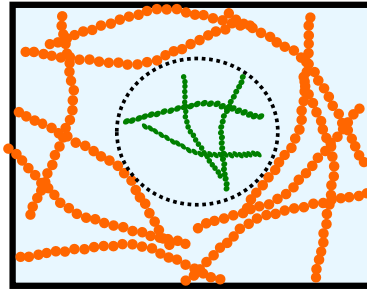866   organization within aggregates.

867   *5.2.3 Composite polymer gels*

868   The rheological properties of the gels that can be produced using a single biopolymer, such as

869   a protein or polysaccharide, are often unsuitable for mimicking the properties of solid animal

870   sourced foods, like meat, seafood, cheese, or cooked egg. This problem can often be overcome

871   by using combinations of different biopolymers. Different kinds of structures can be formed in

872   composite materials formed when two gelling biopolymers are used, depending on the nature of

873   the interactions between them, including interpenetrating, phase-separated, and co-gelling

874   systems (**Figure 12**). Each of these gel types has different physicochemical and functional

875   properties, which provides flexibility in using biopolymers to simulate the rheological properties

876   of solid animal sourced foods.

Interpenetrating Network   **Phase Separated Networks**   **Co-Gelling Networks**
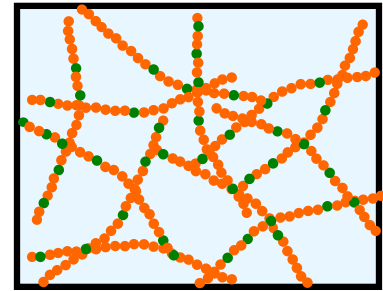
Figure 12: Different kinds of gels can be formed from two biopolymers depending on the interactions involved, including interpenetrating network, phase separated network, and co-gelling networks.

Interpenetrating (IP) networks, which contain two types of biopolymers crosslinked by different gelling mechanisms, may be particularly suitable as meat and seafood analogs. Because they contain two biopolymers that behave differently, they can be designed to have properties that are different from the hydrogels formed using single biopolymers. Studies have shown that hydrogels consisting of interpenetrating networks can be designed to be both strong and ductile (flexible), which are important attributes for simulating the properties of meat and seafood products and is difficult to achieve using single network hydrogels [69, 70]. These kinds of hydrogels contain two biopolymer networks with different attributes: a rigid (strong and brittle) one formed by strongly crosslinked biopolymers and a flexible (soft and ductile) one formed by weakly crosslinked biopolymers [69]. When an external force is applied to this type of IP hydrogel, the crosslinks in the rigid biopolymer network act as sacrificial bonds that are disrupted first, which causes the mechanical energy to be dissipated throughout the system, thereby improving the resistance to crack propagation and fracture. In contrast, the crosslinks in the flexible biopolymer network remain intact, thereby maintaining the overall integrity of the hydrogel. The rigid bonds can then reform when the external force is removed, leading to a strong and resilient hydrogel.

Combinations of two biopolymer networks can also be used to mimic the thermal behavior of meat and seafood products during cooking. When these products are heated, they often undergo an initial softening due to unfolding of the collagen in the connective tissue and then a hardening

901 due to unfolding and aggregation of the muscle proteins. This kind of complex thermal behavior

902 could be mimicked using a combination of cold-set and heat-set biopolymers in IP hydrogels.

903 However, it is important to select the most appropriate types and concentration of biopolymers to

904 obtain an appropriate elastic modulus-temperature profile.

905 *5.2.4. Filled gels*

906 Solid and semi-solid NG-PB foods, like meat, seafood, and egg analogs, often contain

907 inclusions such as fat droplets, protein particles, or starch granules embedded in a biopolymer

908 matrix [1]. The presence of these inclusions impacts the rheological properties of the material by

909 an amount that depends on their size, shape, mechanical properties, aggregation state, and

910 interactions with the surrounding biopolymer matrix [71]. The inclusions may act as active or

911 inactive fillers depending on whether they have strong attractive interactions with the biopolymer

912 matrix or not, respectively (**Figure 13**). Typically, active fillers tend to increase the gel strength

913 whereas inactive ones tend to decrease it [72]. The size of the inclusions relative to the pore size of

914 the biopolymer matrix also impact the overall gel strength [73]. For inactive fillers, inclusions that

915 are smaller than the pore size may not have a major impact on the gel strength because the

916 structure of the biopolymer matrix is not disrupted. In contrast, inclusions larger than the pore

917 size may decrease the gel strength because they disrupt the biopolymer matrix. The shape of the

918 inclusions may also be important because it influences the stress distribution throughout the

919 material. The concentration of the inclusions within a biopolymer matrix also impacts the

920 rheological properties of composite materials. For active fillers, it has been shown that

921 incorporating inclusions up to a certain concentration increases the gel strength but above this

922 concentration is reduces it, which has been attributed to the tendency of high levels of inclusions

923 to disrupt the biopolymer network. Consequently, it is possible to modulate the properties of

924 NG-PB foods by controlling the types and amounts of inclusions present.

INACTIVE FILLER
Particles do not form bonds with polymers
Particles decrease gel strength

ACTIVE FILLER
Particles form bonds with polymers
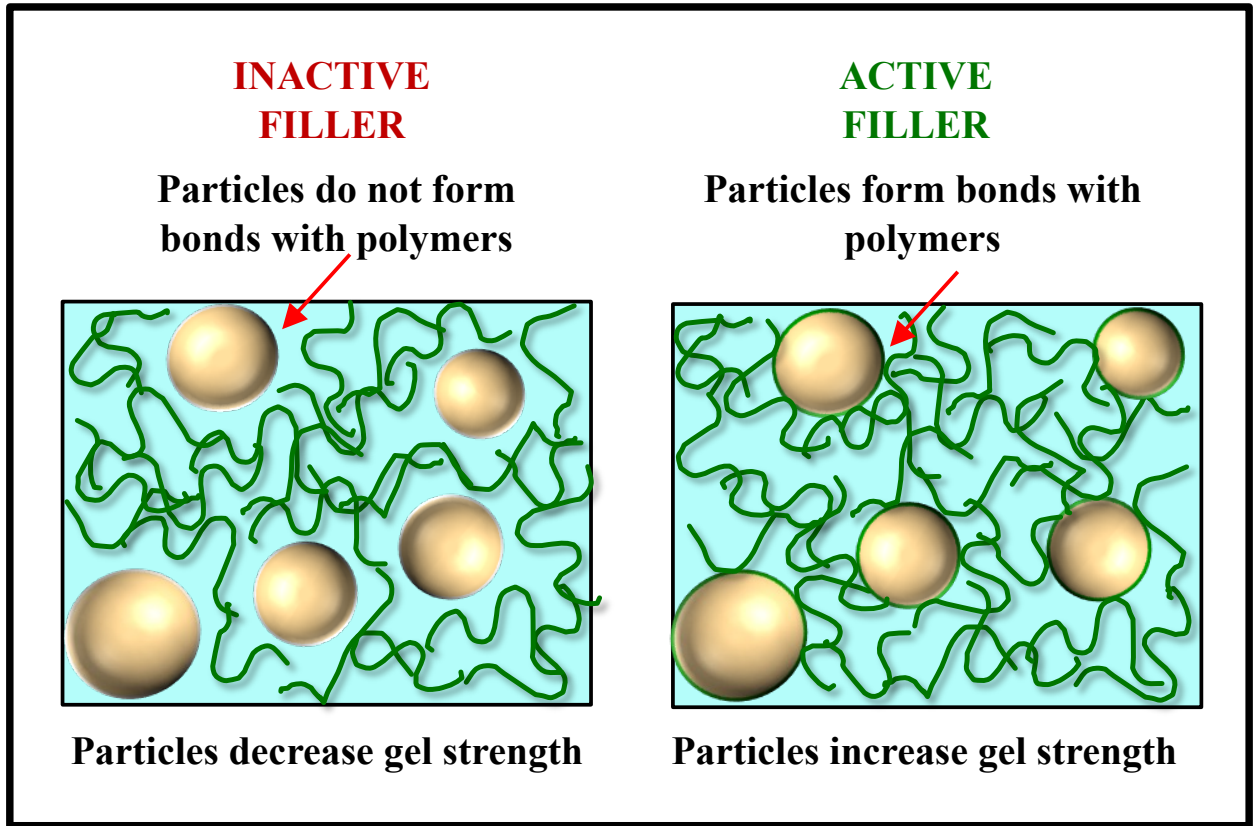Particles increase gel strength

925

Figure 13. Schematic diagram of the structure and interactions of filled gels that container inactive fillers that do not interact strongly with the polymer network, or active fillers that do..

Mathematical models have been developed to describe the impact of inclusions on the properties of gels [74-77]. For instance, the equation below models the impact of active rigid spherical inclusions on the elastic modulus of a polymer matrix [77]:

$$E_C = E_m \left(1 + \frac{15(1-v_m)(M-1)\phi_f}{(8-10v_m)M+7-5v_m-(8-10v_m)(M-1)\phi_f} \right) \qquad (20)$$

Here, $M = E_f/E_m$, and E_C, E_f, and E_m are the elastic moduli of the composite material, the filler particles, and the surrounding matrix, respectively. In addition, v_m is the Poisson ratio (assumed to be 0.5 for gels) and ϕ_f is the volume fraction of particles embedded within the matrix. This model was derived assuming that the particles are active fillers that strongly interact with the polymer matrix. Other models are more appropriate for inactive fillers [71].

In general, the mathematical theories developed to model the mechanical properties of filled gels indicate that the impact of the inclusions depends on their concentration, size, shape, mechanical properties, surface properties, and interactions with the surrounding polymer matrix.

940 This knowledge can be utilized by the manufacturers of NG-PB foods to create products that

941 better simulate those of animal sourced ones.

942 **5.3. Major factors impacting the rheology of colloidal solids**

943   In general, many different factors can impact the rheological behavior of colloidal gels

944 depending on their composition, structure, and interactions. The relative importance of these

945 factors depends on the types and amounts of polymers or particles present, as well as the

946 environmental and solution conditions used. In this section, the power of using theoretical

947 equations to model the properties of colloidal gels is highlighted by showing their ability to

948 identify and quantify the main factors impacting the rheology of these systems. The main focus

949 will be on particle gels since these are often used to formulate meat, seafood, egg, and cheese

950 analogs through controlled assembly of globular plant proteins. The equations developed to

951 model double fractal colloidal particle gels discussed above indicate that their rheology depends

952 on various factors:

953   *Interaction strength (U):* The strength of the attractive interactions between protein

954 molecules may be controlled by altering solution or environmental conditions during gel

955 preparation. Heating proteins above their thermal denaturation temperature promotes unfolding,

956 which exposes non-polar groups, thereby increasing the hydrophobic attraction between them.

957 Conversely, cooling a protein gel formed at a high temperature increases the attractive

958 interactions between the protein molecules due to an increase in the strength of the hydrogen

959 bonding, thereby leading to an increase in gel strength. Most proteins have an electrical charge,

960 which alters the electrostatic interactions with their neighbors. Adding salts or adjusting the pH

961 towards the isoelectric point reduces the magnitude of the electrostatic repulsive interactions

962 between them, which can promote stronger bonds being formed, leading to an increase in gel

963 strength.

964   *Particle concentration* (ϕ): The elastic modulus, yield stress, and yield strain of a colloidal

965 particle gel can also be modulated by altering the particle concentration. The equations based on

966 the double-fractal model predict that the elastic modulus and yield stress increase with increasing

967 particle concentration. Thus, the strength of gels formed from proteins can usually be increased

968 by raising the protein concentration. The full versions of the above equations predict that the

969 yield strain should decrease with increasing particle concentration in the strong-link limit ($\alpha = 1$)

970 but should increase in the weak-link limit ($\alpha = 0$), which was also predicted in earlier models of

971 fractal particle gels [78]. Consequently, measurements of the impact of particle concentration on
972 the yield strain may be a useful method of determining which is the dominant interaction
973 (particle-particle or floc-floc) in the system. This knowledge can then be used to select the most
974 appropriate version of the model to use (*e.g.,* $\alpha = 0$ or 1).

975 *Particle size* (*a and l*): The theoretical equations also provide valuable insights about how the
976 size of the particles (*a*) or flocs (*l*) influence the rheological properties of colloidal particle gels.
977 Typically, the elastic modulus, yield stress, and yield strain all increase as the size of the
978 particles in the system decrease.

979 *Fractal dimensions* (*D and d*): The fractal dimensions of a colloidal particle gel depend on the
980 structural organization of the particles within the flocs, as well as the flocs within the overall
981 system [67]. Typically, the percolation threshold (the minimum particle concentration required to
982 form a gel) decreases as the fractal dimensions decrease., *i.e.,* as the structure becomes more
983 open. Colloidal particle gels where the particle-particle interactions dominate ($\alpha=0$) and the
984 fractal properties of the particles and flocs are similar are used to demonstrate the impact of
985 fractal dimensions on the rheological properties. The shear modulus, yield stress, and yield
986 strain all increase with decreasing fractal dimensions (D_P) for this kind of system. Thus, it may
987 be possible to increase the gel strength by creating structures with a lower fractal dimension.
988 This can be achieved by increasing the strength of the attractive interactions between the
989 particles in the system: the stronger the attraction, the lower the fractal dimension because the
990 particles tend to stick together tightly after contacting each other, thereby leading to a more open
991 structure. In contrast, when the interactions are relatively weak, the particles can reorganize
992 themselves after coming into contact, leading to a more compact structure and higher fractal
993 dimension.

994 Experimentally, it is possible to manipulate many of the properties of particle gels by altering
995 solution or environmental conditions, such as biopolymer concentration, biopolymer type, pH,
996 ionic strength, or temperature. Consequently, it is possible to create plant-based gels with
997 different properties that may be suitable for different applications.

998 **5.4. Examples of rheological properties of solid NG-PB foods**

999 In this section, selected examples of the rheological characterization of solid and semi-solid
1000 NG-PB foods from the author's and other researchers' laboratories are provided to demonstrate
1001 the application of these methods.

1002 *5.4.1. Temperature-sweep experiments*

1003   Temperature-sweep experiments are commonly used to characterize the rheological properties

1004   of solid and semi-solid foods, including those assembled from plant-based ingredients [1]. They

1005   provide valuable insights into the key events that occur during the heating or cooling of foods,

1006   such as thermal denaturation of proteins, helix-coil transitions of polysaccharides, and melting-

1007   crystallization of fats. These experiments are usually carried out using a dynamic shear

1008   rheometer operating in oscillation mode at a fixed frequency and strain (below the linear

1009   viscoelastic region). The test sample is placed in the measurement cell of the rheometer, allowed

1010   to reach the starting temperature, and then heated and/or cooled in a controlled manner. The

1011   dynamic shear modulus is then measured as a function of temperature and the data is plotted as

1012   either the storage (G') and loss (G'') moduli or the complex shear modulus (G^*) and phase angle

1013   (δ) *versus* temperature.

1014   As an example, the thermal gelation of globular proteins is considered because they are often

1015   used to formulate NG-PB meat, seafood, egg, and cheese products. In these applications, an

1016   aqueous protein solution is first prepared by dissolving native globular proteins in water under

1017   appropriate pH and salt conditions. These conditions are selected to ensure the proteins are

1018   initially soluble before heating but will form an irreversible heat-set gel during heating.

1019   Typically, the electrostatic interactions in the protein solution are modulated by controlling the

1020   pH and ionic strength. The solution is then heated to a temperature above the thermal

1021   denaturation temperature of the proteins, which causes them to unfold and aggregate with their

1022   neighbors, which is mainly driven by the increased hydrophobic attraction that arises when non-

1023   polar groups are exposed at the surfaces of the denatured protein molecules. If the protein

1024   concentration is sufficiently high, then the aggregated proteins form a 3D network that occupies

1025   the entire volume of the sample, leading to elastic-like properties. To accurately simulate their

1026   quality attributes and cooking properties, the gelation temperature and final gel strength of NG-

1027   PB foods should be as similar as possible to those of the animal sourced foods they are intended
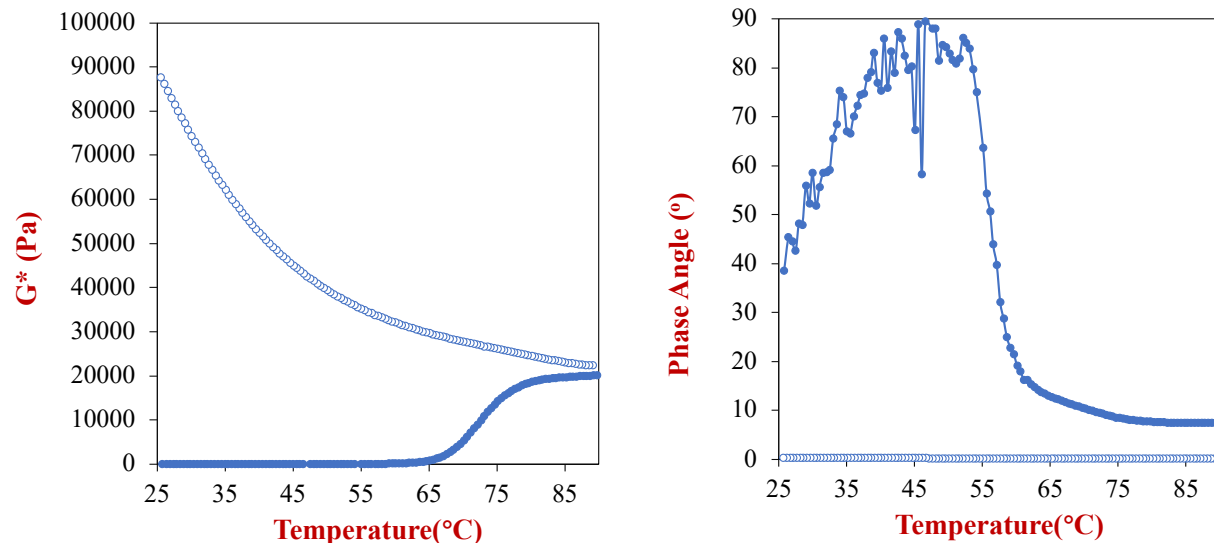
1028   to replace (such as egg or meat).

1029

An example of the rheological behavior of a 20 wt% potato protein solution (pH 7) during heating and cooling is shown in **Figure 14**. The rheology was characterized by measuring the dynamic shear modulus *versus* temperature at a fixed frequency (1 Hz) and strain (1%), which was in the linear viscoelastic region. The complex shear modulus (G*) and phase angle (δ) are plotted versus temperature during heating and cooling. Initially, the shear modulus was relatively low because the protein molecules were in their native state and did not associate strongly with each other because of the relatively strong electrostatic repulsion between them **(Figure 14a)**. However, when they were heated above about 65°C, the shear modulus increased steeply, which can be attributed to protein unfolding and aggregation around the thermal denaturation temperature of the potato proteins, thereby leading to a 3D elastic network being formed. The shear modulus then increased slightly when the system was heated further, which was probably because more protein molecules unfolded and participated in network formation. When the protein gels were cooled, there was a pronounced increase in the shear modulus, which can be attributed to strengthening of the hydrogen bonding between the protein molecules in the gel network.

The phase angle was initially around 40°, which suggested that the protein dispersions exhibited a small amount of elasticity, perhaps due to some weak attractive interactions between
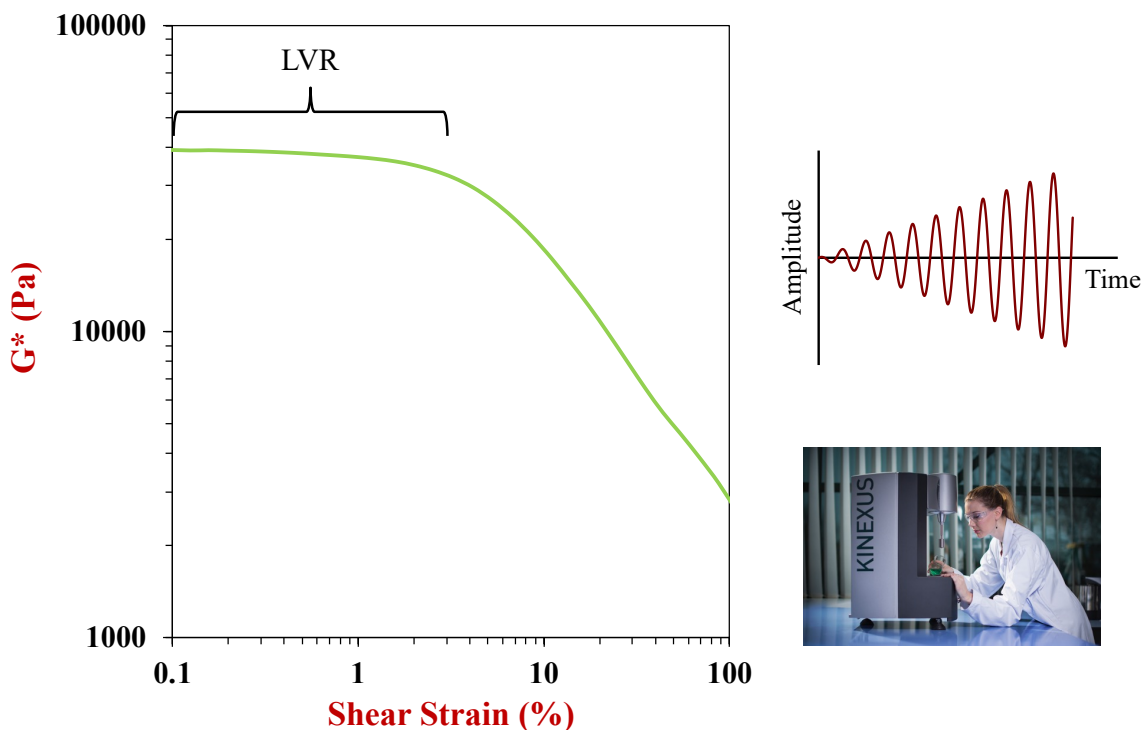
the proteins (**Figure 14b**). During heating, the phase angle first increased above 45°, which suggested that this weak network dissociated so the proteins became more mobile, thereby leading to a more fluid-like behavior. However, once the temperature exceeded about 65 °C, there was a steep decrease in the phase angle, which can be attributed to the formation of a 3D network of aggregated protein molecules that provide some elasticity. The phase angle remained low during further heating and cooling, which indicates that the protein gels formed retained their strongly elastic properties. As mentioned earlier, it is often important to mimic the gelling temperature and final gel strength of animal-sourced products.

In general, these kinds of measurements can be used to determine the impact of different additives and other variables on the gelation temperature and gel strength of plant-based foods, including protein type, protein concentration, salt content, pH, polysaccharide type, and polysaccharide concentration. In addition, they can be used to compare the thermal behavior of NG-PB foods to that of animal sourced foods, which may be useful for simulating their cooking behavior. As an example, temperature sweep measurements of the shear modulus *versus* temperature have been used to assess the suitability of a globular plant protein derived from duckweed (Rubisco) for simulating the cooking and textural attributes of globular egg white proteins from hen's egg [54]. In another study, these measurements were used to characterize changes in the texture of salmon during heating, with the aim of providing information that could be used to formulate better plant-based seafood analogs [79]. They have also been used to characterize the textural properties of plant-based adipose tissue formulated from high internal phase oil-in-water emulsions during heating and cooling [17]. Other researchers have used this approach to characterize the properties of gels made from quinoa flour, which were produced for potential application in formulating NG-PB meat analogs [80].

5.4.2. Strain-sweep experiments

Strain-sweep experiments are also commonly used to characterize the rheological properties of solid or semi-solid colloidal foods. These experiments are usually carried out using a dynamic shear rheometer operating in oscillation mode at a fixed frequency. In these experiments, the test sample is placed in the measurement cell of the rheometer and allowed to equilibrate to the measurement temperature. An oscillating stress is then applied whose magnitude is incrementally increased over time (**Figure 15**), and then the magnitude and phase of the resulting oscillating strain is recorded. The dynamic shear modulus (G'/G" or G*/δ) is then plotted as a

1085   function of increasing stress or strain.

Figure 15. The complex shear modulus of a material measured using dynamic shear rheometry is often linear up to a critical strain and then decreases steeply. The region where the modulus remains constant is known as the linear viscoelastic regime (LVR). This is a curve for a plant-based chicken sample made in our laboratory. Figure of rheometer kindly supplied by Netsch.

As an example, the change in shear modulus with applied strain for heat-set potato protein gels is shown in **Figure 15**. The elastic modulus remains relatively constant at low shear strains but then decreases substantially when a particular strain is exceeded, which may be taken to indicate yielding. The yield stress and yield strain can then be obtained from this point. Upon a further increase in applied stress, there may be a further steep decrease in the elastic modulus, which is indicative of fracturing of the gel. The fracture stress and strain can then be obtained from this point.

The impact of the magnitude of the applied strain on the dynamic shear rheology of peanut protein gels has been characterized using this method [81]. This study found that the shear modulus remained relatively constant at low applied strains (< LVR) but decreased appreciably once the strain exceeded about 1%. They also found that the storage modulus was greater than the shear modulus (G'>G") across the entire strain range studied (0.01 to 10%). Strain sweeps

1104   have also been used to compare the rheological properties of plant protein gels (zein or gluten)

1105   with those of animal sourced foods (like real cheese and chicken) [82]. Again, the shear modulus

1106   of all samples remained relatively constant at low strains but decreased steeply when a particular

1107   strain was exceeded. However, there were appreciable differences between the samples. For

1108   instance, the yield strain of the zein gels was appreciably lower than that of chicken but fairly

1109   similar to that of cheese, which impacts the kinds of NG-PB foods zein gels can be applied in.

1110   Strain sweep experiments have also been used to characterize the rheology of plant protein

1111   doughs, such as those formulated from potato, pea, or soy protein, which may form a basis for

1112   formulating some NG-PB foods [83].

1113   *5.4.3. Frequency-sweep experiments*

1114   Useful information about the textural attributes of solid or semi-solid foods can often be

1115   obtained by measuring changes in their rheological properties when the frequency of the

1116   oscillating shear stress applied to them is increased. Again, these experiments are typically

1117   carried out using a dynamic shear rheometer. The test sample is placed in the measurement cell

1118   of the instrument, allowed to real the target temperature, and then an oscillating stress of

1119   progressively increasing frequency is applied at a fixed strain (within the LVR). The dynamic

1120   shear modulus (G'/G" or G*/δ) is then plotted as a function of increasing frequency. This kind

1121   of experiment can provide valuable insights into the dynamic processes occurring within

1122   materials under stress, such as changes in the structural organization of the polymers or particles

1123   they contain, which can be characterized by relaxation times or frequencies. For instance, the

1124   time for polymers or particles within a gel network to rearrange themselves when a stress is

1125   applied can be determined, which provides insights into the characteristics of these structural

1126   elements. The relaxation frequency (f_R) is taken to be the point where the elastic and storage

1127   modulus crossover each other (G'=G") when the frequency is increased, which can then be

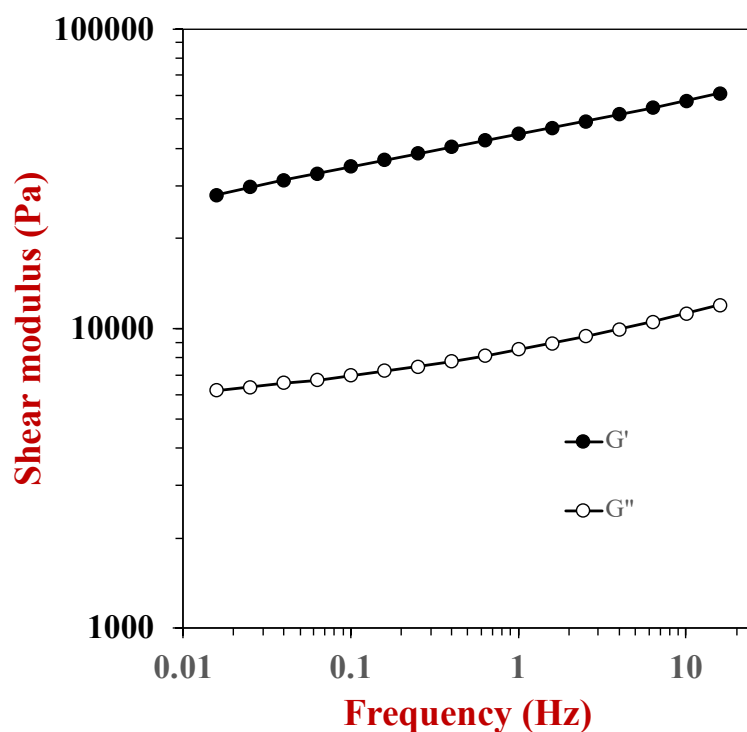1128   converted to a relaxation time ($t_R = 1/f_R$).

1129

Figure 16. Influence of applied frequency on the storage (G') and loss (G") moduli of 10 wt%
potato protein gels (pH 7) measured at a strain of 1% (in linear viscoelastic regime) at 25 $^{\circ}$C.
(Data kindly supplied by Hualu Zhou).

Measurements of the shear modulus *versus* frequency profile for a heat-set plant-protein gel is
shown in **Figure 16**. In this case, the storage modulus was greater than the loss modulus across
the entire frequency range studied, which indicated that the gels were always predominantly
elastic. There was a slight increase in both the storage and loss moduli as the frequency was
raised, which may be because the structural entities formed by the proteins in the gels had less
time to respond to the applied oscillating stress at higher frequencies, so there was more
resistance to deformation. Other researchers have characterized the dynamic shear rheology of
peanut protein gels using this approach [81]. They also reported an increase in shear modulus
when the frequency was raised, and that the storage modulus was always higher than the loss
modulus over the frequency range studied (0.1 to 10 Hz). The frequency dependence of plant
polysaccharide (fenugreek gum) gels has also been characterized using this approach [84]. At low
frequencies, G" > G', which indicated that the polysaccharide solutions were predominantly
fluid-like. When the frequency was raised, both G' and G" increased but there was a crossover

1147   point (G'=G") at an intermediate frequency, after which G'>G", indicating that the gels became

1148   more solid-like at higher frequencies. These gels could therefore be characterized by a

1149   relaxation time. At low frequencies, there was sufficient time for the polysaccharide molecules

1150   to rearrange when an oscillating stress was applied, leading to fluid-like behavior. In contrast, at

1151   high frequencies, there was insufficient time for these molecules to rearrange, leading to more

1152   resistance to deformation and solid-like behavior. The relaxation frequency was found to

1153   decrease with increasing polysaccharide concentration, which can be attributed to the fact that

1154   the greater entanglements and interactions of the polysaccharide molecules in more concentrated

1155   systems inhibits their movement. These kinds of frequency sweep tests can therefore provide

1156   valuable information about the dynamic properties of the biopolymer gels used to formulate

1157   some NG-PB foods.

1158   *5.4.4. Large deformation experiments*

1159   In many practical applications, it is important to understand how NG-PB foods behave when

1160   they undergo large deformations. For instance, the cutting of meat, the slicing of cheese, the

1161   scrambling of eggs, or the mastication of solid foods all involve large deformations of the

1162   material, which cause the food structure to become disrupted. Consequently, it is important to

1163   characterize the rheological behavior of NG-PB foods exposed to large stresses and strains. In

1164   this section, we provide examples of some of the most common experimental approaches used to

1165   obtain this kind of information for these foods.

1166   *Large amplitude oscillatory shear (LAOS):* LAOS experiments are typically carried out using

1167   a dynamic shear rheometer [85, 86]. The test sample is placed in the measurement cell and then an

1168   oscillating shear stress that progressively increases in amplitude is applied. This test is therefore

1169   similar to the strain-sweep tests described earlier (Section 6.2.4.2). However, LAOS

1170   experiments focus on the behavior of the material within the larger deformation regime, rather

1171   than the transition from the linear to non-linear viscoelastic regimes. Because the stress-strain

1172   and stress-strain rate relationships are non-linear at high deformations specialized mathematical

1173   approaches are needed to interpret and represent the data [85, 86]. This is mainly because second

1174   and higher order harmonics contribute to the rheological properties of the material in the non-

1175   linear regime, whereas only first-order harmonics contribute in the linear regime [86, 87].

1176   Information about the transient behavior of a material under large deformation can be obtained

1177   by plotting Lissajous curves, which show the stress *versus* strain relationship for the elastic

1178　component and the stress *versus* strain rate profile for the viscous component of the shear

1179　modulus (**Figure 17**). The shape of these curves provides insights into the nature of the material

1180　being tested, such as viscous, elastic, viscoelastic, or plastic. The energy dissipation per unit

1181　volume of material per oscillation cycle can be calculated from the area under the Lissajous

1182　curves, which provides useful insights into the impact of deformation on structural and textural

1183　changes [88, 89].

1184
1185
1186　**Figure 17.** Highly schematic representation of the different kinds of Lissajous plots that can be
1187　obtained for different materials. In practice, other shapes can be seen for more complex
1188　materials, especially during large deformation measurements.
1189

1190　　The LAOS method has been used to test several model plant-based foods. For instance, it

1191　was used to quantify the impact of gum concentration on the rheology of soy protein isolate -

1192　carboxymethyl flaxseed gum (SPI-CMFG) mixtures [90]. The authors reported that the storage

1193　modulus, loss modulus, and apparent shear viscosity of the SPI-CMFG mixtures increased with

1194　increasing CMFG concentration. Other researchers utilized both small and large amplitude

1195　oscillatory shear (SAOS and LAOS) tests to characterize the impact of composition on the

1196　rheology of konjac glucomannan solutions at low and high deformations [91]. The storage

1197　modulus, loss modulus, and apparent viscosity of the konjac glucomannan solutions increased

1198　with increasing polymer concentration but decreasing NaCl concentration. The LAOS tests

1199　showed that increasing the konjac glucomannan concentration changed the shape of the

1200　Lissajous plots, which provided insights into changes in the conformation and interactions of the

1201　polysaccharides. In another study, researchers used LAOS to study the suitability of blends of

1202　plant proteins (soy or pea proteins) and polysaccharides (cellulose or pectin) for formulating

1203　meat analogs [88]. The polysaccharide-protein composites had more fibrous structures than protein

1204　alone, which could be useful for mimicking the structural and textural attributes of real meat.

1205   LAOS testing was used to provide information about changes in the rheology of the protein-

1206   polysaccharide composites when their compositions were changed. The same authors used this

1207   method to test the impact of thermal processing on the properties of plant protein gels formed

1208   from pea, soy, or wheat gluten proteins [89]. SAOS and LAOS tests have also been used to

1209   characterize the rheological properties of plant-based edible inks suitable for 3D food printing

1210   applications [92]. These edible inks were prepared by blending soy protein with either guar gum or

1211   xanthan gum to achieve the required printing characteristics.

1212   *Large-deformation compression tests*: The mechanical properties of materials at large

1213   deformations are often assessed using compression tests. Typically, a test material of fixed

1214   shape and dimensions, such as a cylinder of known height and diameter, is placed on the

1215   measurement cell of the instrument. The force acting on a probe as it compresses the test

1216   material at a fixed speed is then measured over time. This information is used to calculate the

1217   relationship between the applied stress and the resulting strain of the material (**Figure 9**). At low

1218   deformations, the stress is proportional to the strain and the elastic modulus can be calculated

1219   from the initial slope. However, at higher deformations the material may exhibit some flow or

1220   disruption, and so the stress is no longer proportional to the strain. In the case of fracturing, the

1221   fracture stress and fracture strain can be determined as the point where there is an obvious break

1222   in the stress-strain relationship. These parameters can then be plotted on a 2D plot of critical

1223   stress *versus* critical strain to provide insights into the textural attributes of the test material

1224   (**Figure 9**). Typically, the material can be classified as brittle, tough, mushy, or rubbery

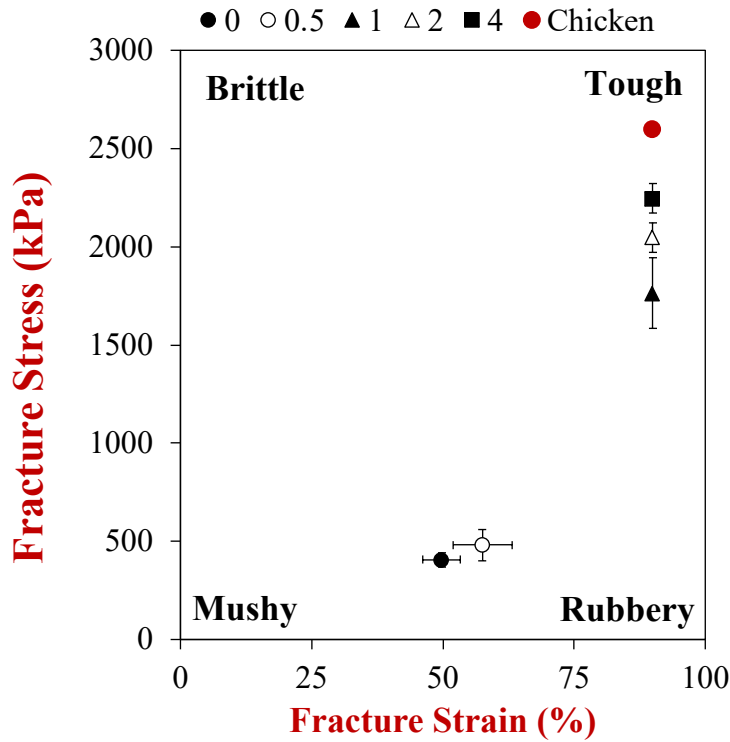1225   depending on where it falls on the texture map [88].

Figure 18. A 2D Texture map can be used to characterize the fracture properties of NG-PB foods and compare them to real ones. In this case, the fracture stress and strain of several plant-based chicken formulations (which consisted of 10% potato protein and 0, 0.5, 1, 2, o4 4% gellan gum) are compared to those of real chicken. Data kindly provided by Hualu Zhou.

As an example, our laboratory has used this approach to compare the properties of plant-based chicken analogs to real chicken (**Figure 18**). The chicken analogs were prepared by preparing a series of potato protein-gellan gum composite gels with different compositions. The textural attributes of the chicken analogs could be manipulated to be somewhat similar to those of real chicken by using sufficiently high concentrations of plant protein and polysaccharide. These kinds of texture maps can also be developed by measuring the stress and strain of plant-based composites using a dynamic shear rheometer, where the critical stress and strain at the end of the linear viscoelastic region are used [88].
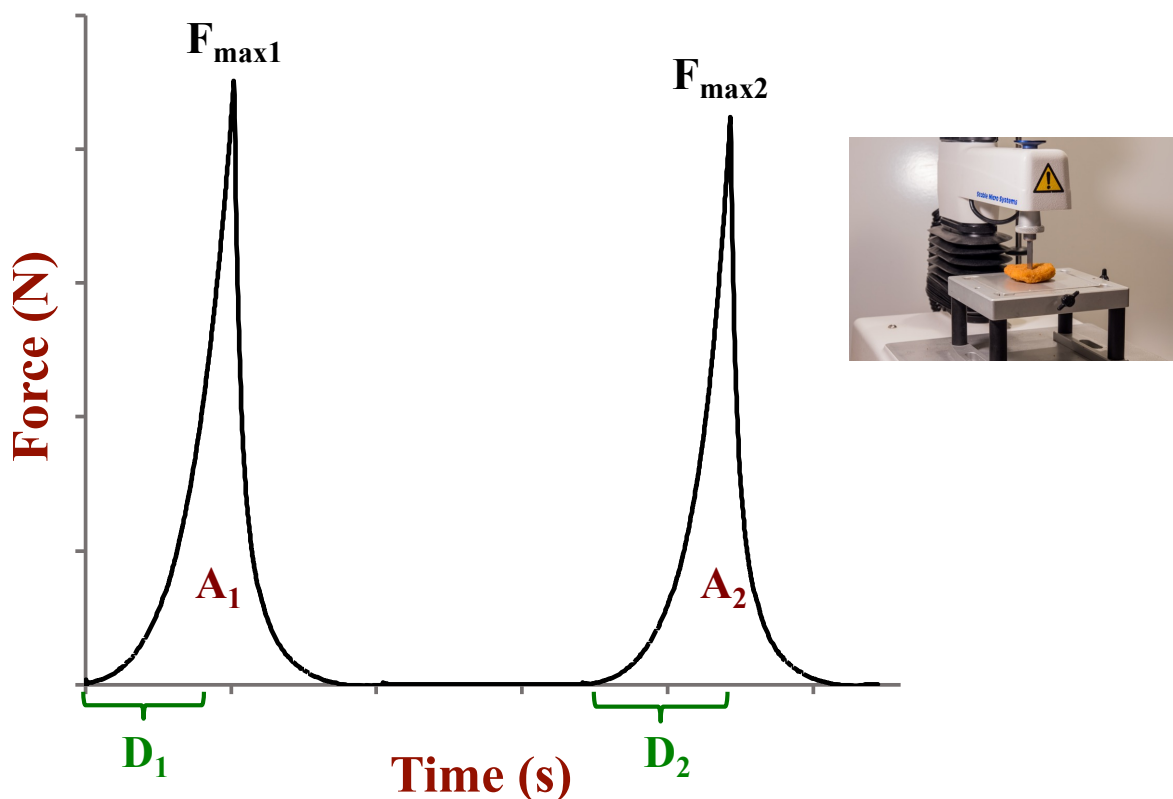
Figure 19. The rheology of solid or semi-solid NG-PG foods is often characterized by texture profile analysis (TPA), which involves compressing/decompressing the sample twice and measuring the force versus time or distance. Measurement probes with different sizes and shapes can be used to mimic practical situations. Representative measurements are shown that are used to determined TPA parameters, such as forces, areas, and distances. Image of instrument kindly supplied by Texture Technologies Corporation.

Texture profile analysis: The TPA method is probably the most common approach for characterizing the large deformation behavior of solid and semi-solid foods, including NG-PB foods [1]. As mentioned earlier, a test sample with a well-defined size and shape (such as a cylinder) is placed on the measurement cell and then the sample is compressed-decompressed twice (Section 5.2.1.1). The change in the force with time (or deformation) is then recorded and analyzed (**Figure 19**). Various textural parameters can then be calculated from the height, position, and area of the two peaks obtained during the double compression-decompression cycle, such as the hardness, fracturability, cohesiveness, springiness, resilience, gumminess, and chewiness (**Table 2**). Ideally, the parameters measured for a NG-PB food should match those of the animal sourced food it is designed to replace. This method can therefore be used to determine the impact of different parameters on the textural attributes of NG-PB foods such as

1259 their composition or preparation method, as well as to compare the properties of NG-PB foods to

1260 those of animal sourced foods.

1261   The TPA method has been used in our laboratory to compare the properties of real

1262 beefburgers with several plant-based ones [93, 94]. The TPA parameters determined using a double

1263 compression-decompression test are summarized in **Table 5**. Radar plots of selected PB burgers

1264 are shown in **Figure 20**, which compare the percentage of each TPA parameter to that found for

1265 real beefburgers (100%). Notably, there were large differences between the textural attributes of

1266 the NG-PB burgers and the real beefburgers, which would be expected to lead to sensory

1267 differences. These results highlight the need for further research to better simulate the textural

1268 attributes of real meat using plant-based meat analogs.

1269

1270   **Table 5.** Comparison of the TPA parameters of several commercial plant-based (PB) burgers

1271 with those of real beef burgers. Data taken from experiments in our laboratory [94].

1272

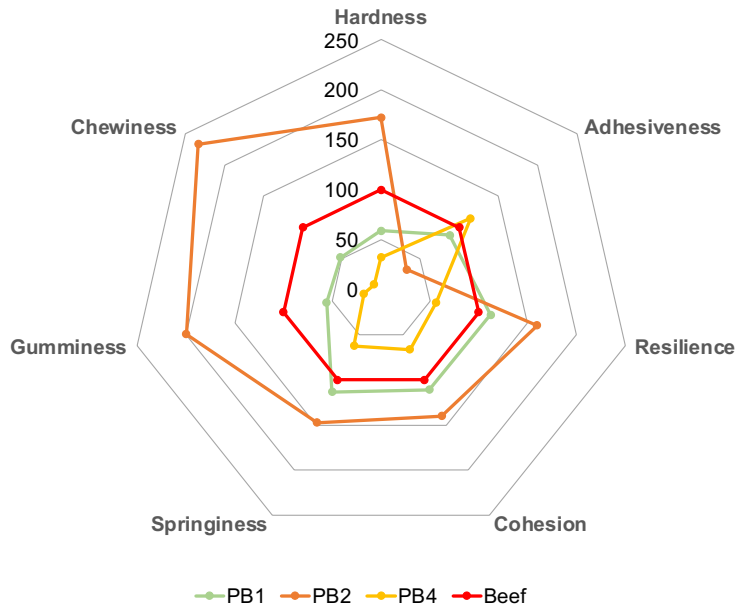|	PB1	PB2	PB3	PB4	PB5	Beef
Hardness (g)	440 ± 80	1300 ± 250	1500 ± 180	240 ± 29	270 ± 21	2400 ± 450
Adhesiveness (g.sec)	-0.91 ± 0.77	-0.34 ± 0.27	-1.2 ± 0.65	-1.2 ± 0.60	-1.6 ± 0.65	-0.47 ± 0.19
Resilience (%)	14 ± 3.4	20 ± 1.6	16 ± 1.0	7.2 ± 0.87	5.8 ± 0.68	24 ± 1.3
Cohesion	0.41 ± 0.07	0.52 ± 0.03	0.46 ± 0.02	0.24 ± 0.02	0.21 ± 0.02	0.61 ± 0.02
Springiness (%)	61 ± 11	79 ± 5.0	64 ± 3.2	34 ± 3.5	32 ± 3.8	88 ± 2.8
Gumminess	190 ± 64	660 ± 120	700 ± 94	59 ± 7.1	57 ± 8.0	1400 ± 270
Chewiness	120 ± 58	530 ± 120	450 ± 62	20 ± 3.6	18 ± 4.0	1300 ± 250

1273

1274

Figure 20. Comparison of the TPA parameters of several commercial plant-based (PB) burgers with those of real beef burgers. Data taken from experiments in our laboratory (Zhou, et al., 2022a).

Many other researchers have also used TPA to characterize the rheological properties of model or commercial plant-based foods. For instance, this method has been used to establish the impact of a dietary fiber (psyllium) on the textural attributes of plant-based sausages [95]. The researchers found that the addition of the dietary fiber increased the firmness, hardness, springiness, cohesiveness, resilience, and chewiness of the plant-based sausages, which altered their sensory attributes. In another study, TPA was used to characterize the effects of sweet potato starch and konjac glucomannan on the textural attributes of plant-based pork rinds formulated from emulsion gels composed of soy protein and soy oil [96] The hardness, cohesiveness, and chewiness of the pork rind analogs could be optimized by controlling the amounts of starch and glucomannan added. TPA has also been used to characterize the impact of formulation and processing parameters on the creation of various other plant-based foods, including the addition of methylcellulose on beefburger analogs [97], the addition of apricot seed extract on kefir analogs [98], and the impact of heating and cooling on pork back fat analogs [99].

6. Conclusions

There has been a surge of interest in the creation of NG-PB foods that accurately simulate the properties of traditional animal-based products, like meat, seafood, egg, and dairy products.

1296 These products exhibit a broad diversity of rheological characteristics, including low viscosity

1297 fluids (like milk), high viscosity fluids (creams), soft solids (like yogurt), and hard solids (like

1298 some cheeses). Moreover, solid or semi-solid products may be expected to be brittle, rubbery,

1299 mushy, or tough depending on their nature. Consequently, it is important for the manufacturers

1300 of NG-PB foods to be able to mimic this broad range of products. This requires the availability

1301 of analytical methods to quantify and compare the properties of foods, as well as mathematical

1302 models to identify the key factors that impact their textural attributes.

1303 In this article, it was shown that most NG-PB foods can be considered to be fluid, semi-

1304 solid, or solid colloidal dispersions consisting of polymers and/or particles dispersed in an

1305 aqueous medium. Consequently, their rheological properties can be measured and modelled

1306 using the analytical techniques and theoretical equations that have been developed to describe

1307 colloidal dispersions. It has been demonstrated that identifying an appropriate theoretical model

1308 can provide valuable insights into the relative importance of different parameters that impact the

1309 rheological attributes of NG-PB foods. These models can therefore be used to optimize the

1310 design of products with improved textural properties. In the future, it will be important to

1311 establish the most appropriate models for different categories of NG-PB foods and to determine

1312 their range of applications. Moreover, it will be useful to tabulate the characteristics of a wide

1313 range of NG-PB foods using standardized methods so that useful comparisons can be made with

1314 other products.

References

1320 1. D. J. McClements and L. Grossmann, *Next-generation Plant-based Foods: Design,*
1321 *Production, and Properties*, Springer, New York, NY, 2022.
1322 2. D. J. McClements and L. Grossmann, *Comprehensive Reviews in Food Science and Food*
1323 *Safety*, 2021, **20**, 4049-4100.
1324 3. K. Kyriakopoulou, B. Dekkers and A. J. van der Goot, *Plant-Based Meat Analogues*, 2019.
1325 4. J. Mewis and N. J. Wagner, *Colloidal Suspension Rheology*, Cambridge Univeristy Press,
1326 New York, 2012.
1327 5. T. A. Vilgis, *Reports on Progress in Physics*, 2015, **78**.

1328   6.   A. Boire, D. Renard, A. Bouchoux, S. Pezennec, T. Croguennec, V. Lechevalier, C. Le
1329   Floch-Fouere, S. Bouhallab and P. Menut, in *Annual Review of Food Science and*
1330   *Technology, Vol 10*, eds. M. P. Doyle and D. J. McClements, 2019, vol. 10, pp. 521-539.
1331   7.   R. G. M. van der Sman, *Advances in Colloid and Interface Science*, 2012, **176**, 18-30.
1332   8.   S. Jeske, E. Zannini and E. K. Arendt, *Plant Foods for Human Nutrition*, 2017, **72**, 26-33.
1333   9.   D. J. McClements, E. Newman and I. F. McClements, *Comprehensive Reviews in Food*
1334   *Science and Food Safety*, 2019, **18**, 2047-2067.
1335   10.   X. Kong, Z. Q. Xiao, M. D. Du, K. T. Wang, W. Yu, Y. H. Chen, Z. L. Liu, Y. Q. Cheng
1336   and J. Gan, *Gels*, 2022, **8**.
1337   11.   L. Sen and S. Okur, *Food Chemistry*, 2023, **402**.
1338   12.   M. Montemurro, E. Pontonio, R. Coda and C. G. Rizzello, *Foods*, 2021, **10**.
1339   13.   L. Grossmann and D. J. McClements, *Trends in Food Science & Technology*, 2021, **118**,
1340   207-229.
1341   14.   E. C. Short, A. J. Kinchla and A. A. Nolden, *Foods*, 2021, **10**.
1342   15.   K. Kyriakopoulou, J. K. Keppler, A. J. van der Goot and R. M. Boom, in *Annual Review of*
1343   *Food Science and Technology, Vol 12, 2021*, eds. M. Doyle and D. J. McClements, 2021,
1344   vol. 12, pp. 29-50.
1345   16.   K. Younis, A. Ashfaq, A. Ahmad, Z. Anjum and O. Yousuf, *Journal of Texture Studies*,
1346   2023, DOI: 10.1111/jtxs.12704.
1347   17.   X. Y. Hu and D. J. McClements, *Journal of the American Oil Chemists Society*, 2022, **99**,
1348   78-78.
1349   18.   X. Y. Hu and D. J. McClements, *Innovative Food Science & Emerging Technologies*, 2022,
1350   **78**.
1351   19.   X. Y. Hu, H. L. Zhou and D. J. McClements, *Food Structure-Netherlands*, 2022, **33**.
1352   20.   R. A. Nicholson and A. G. Marangoni, *Current Opinion in Food Science*, 2022, **43**, 1-6.
1353   21.   J. X. Guo, L. J. Cui and Z. Meng, *Food Hydrocolloids*, 2023, **137**.
1354   22.   Z. Lu, Y. Liu, Y. E. J. Lee, A. Chan, P. R. Lee and H. S. Yang, *Food Chemistry*, 2023, **403**.
1355   23.   G. Vu, X. Xiang, H. Zhou and D. J. McClements, *Foods*, 2023, **12**, 2.
1356   24.   R. C. F. de Menezes, Q. C. D. Gomes, B. S. de Almeida, M. F. R. de Matos and L. C. Pinto,
1357   *International Journal of Gastronomy and Food Science*, 2022, **30**.
1358   25.   J. Hao, X. Y. Li, Q. Y. Wang, W. W. Lv, W. G. Zhang and D. X. Xu, *Journal of the*
1359   *American Oil Chemists Society*, 2022, **99**, 635-653.
1360   26.   F. Zaaboul, Q. L. Zhao, Y. J. Xu and Y. F. Liu, *Food Hydrocolloids*, 2022, **124**.
1361   27.   E. Bertoft, *Agronomy-Basel*, 2017, **7**.
1362   28.   F. Flach, L. Fries, J. Kammerhofer, J. Hesselbach, B. Finke, C. Schilde, G. Niederreiter, S.
1363   Palzer, S. Heinrich and A. Kwade, *Advanced Powder Technology*, 2019, **30**, 2823-2831.
1364   29.   O. G. Jones and D. J. McClements, *Comprehensive Reviews in Food Science and Food*
1365   *Safety*, 2010, **9**, 374-397.
1366   30.   D. Saglam, P. Venema, E. van der Linden and R. de Vries, *Current Opinion in Colloid &*
1367   *Interface Science*, 2014, **19**, 428-437.
1368   31.   M. Li, V. D. Daygon, V. Solah and S. Dhital, *Critical Reviews in Food Science and*
1369   *Nutrition*, 2022, DOI: 10.1080/10408398.2021.1992607.
1370   32.   Y. Ai and J. L. Jane, *Starch-Starke*, 2015, **67**, 213-+.
1371   33.   S. Samard and G. H. Ryu, *Journal of the Science of Food and Agriculture*, 2019, **99**, 2708-
1372   2715.
1373   34.   I. J. Joye and D. J. McClements, *Current Opinion in Colloid & Interface Science*, 2014, **19**,

417-427.

35. N. Reddy and M. Rapisarda, *Materials*, 2021, **14**.
36. M. Miriani, M. Keerati-u-rai, M. Corredig, S. Iametti and F. Bonomi, *Food Hydrocolloids*, 2011, **25**, 620-626.
37. T. G. Burger and Y. Zhang, *Trends in Food Science & Technology*, 2019, **86**, 25-33.
38. D. Iwanaga, D. A. Gray, I. D. Fisk, E. A. Decker, J. Weiss and D. J. McClements, *Journal of Agricultural and Food Chemistry*, 2007, **55**, 8711-8716.
39. K. Hu and D. J. McClements, *Food Hydrocolloids*, 2015, **44**, 101-108.
40. E. ten Grotenhuis, M. Paques and G. A. van Aken, *Journal of Colloid and Interface Science*, 2000, **227**, 495-504.
41. Y. R. Tang and S. Ghosh, *Food Hydrocolloids*, 2021, **113**.
42. T. Tran and D. Rousseau, *Food Hydrocolloids*, 2013, **30**, 382-392.
43. B. Du, S. P. Nie, F. Peng, Y. D. Yang and B. J. Xu, *Food Frontiers*, 2022, **3**, 631-640.
44. L. Sha and Y. L. L. Xiong, *Trends in Food Science & Technology*, 2020, **102**, 51-61.
45. X. Yang, A. Q. Li, X. X. Li, L. J. Sun and Y. R. Guo, *Trends in Food Science & Technology*, 2020, **102**, 1-15.
46. A. J. Stephen, G. O. Phillips and P. A. Williams, *Food Polysaccharides and Their Applications*, CRC Press, Boca Raton, FL., Second Edition edn., 2017.
47. M. Q. Guo, X. Hu, C. Wang and L. Ai, in *Solubility of Polysaccharides*, ed. Z. Xu, IntechOpen, On-line, 2017, DOI: https://www.intechopen.com/books/solubility-of-polysaccharides, ch. Chapter 2, pp. 1-17.
48. D. J. McClements, *Food Emulsions: Principles, Practice, and Techniques*, CRC Press, Boca Raton, 2nd edn., 2015.
49. D. Quemada and C. Berli, *Advances in Colloid and Interface Science*, 2002, **98**, 51-85.
50. R. J. Hunter, *Introduction to Modern Colloid Science*, Oxford University Press, Oxford, U.K., 1994.
51. D. B. Genovese, J. E. Lozano and M. A. Rao, *Journal of Food Science*, 2007, **72**, R11-R20.
52. D. J. McClements, *Food Hydrocolloids*, 2000, **14**, 173-177.
53. T. D. Panaite, S. Mironeasa, M. Iuga and P. A. Vlaicu, *Emirates Journal of Food and Agriculture*, 2019, **31**, 304-314.
54. H. L. Zhou, G. Vu and D. J. McClements, *Journal of the American Oil Chemists Society*, 2022, **99**, 169-169.
55. J. L. Briggs and J. F. Steffe, *Journal of Texture Studies*, 1997, **28**, 517-522.
56. M. A. Rao, *Rheology of Fluid, Semisolid, and Solid Foods: Principles and Applications*, Springer Science, New York, N.Y., Third Edition edn., 2013.
57. T. F. Tadros, *Rheology of Dispersions: Principles and Applications*, Wiley-VCH, Weinheim, Germany, 2010.
58. P. Walstra, *Physical Chemistry of Foods*, Marcel Decker, New York, NY., 2003.
59. T. van Vliet, *Rheology and Fracture Mechanics of Foods*, CRC Press, Boca Raton, FL, 2013.
60. N. Grasso, L. Alonso-Miravalles and J. A. O'Mahony, *Foods*, 2020, **9**.
61. M. J. Hernandez, J. Dolz, J. Delegido, C. Cabeza and M. Dolz, *Journal of Dispersion Science and Technology*, 2008, **29**, 213-219.
62. Y. P. Cao and R. Mezzenga, *Nature Food*, 2020, **1**, 106-118.
63. C. P. Broedersz and F. C. MacKintosh, *Reviews of Modern Physics*, 2014, **86**, 995-1036.
64. T. Funami, S. Noda, M. Nakauma, S. Ishihara, R. Takahashi, S. Al-Assaf, S. Ikeda, K.

1420   Nishinari and G. O. Phillips, *Journal of Agricultural and Food Chemistry*, 2008, **56**,
1421   8609-8618.

1422 65. P. J. Lu and D. A. Weitz, in *Annual Review of Condensed Matter Physics, Vol 4*, ed. J. S.
1423   Langer, 2013, vol. 4, pp. 217-233.

1424 66. A. D. Dinsmore, in *Experimental and computational techniques in soft condensed matter*
1425   *physics*, ed. J. Olafsen, Cambridge University Press, Cambridge, UK, 2010, ch. Chapter
1426   3, pp. 62-96.

1427 67. L.-V. Bouthier, R. Castellani, E. Hachem and R. Valette, *Physics of Fluids*, 2022, **34**,
1428   083105.

1429 68. E. Dickinson, *Advances in Colloid and Interface Science*, 2013, **199**, 114-127.

1430 69. S. Bi, J. Pang, L. Huang, M. Sun, X. Cheng and X. Chen, *International journal of biological*
1431   *macromolecules*, 2020, **146**, 99-109.

1432 70. P. P. Zhu and Z. Zhong, *Mechanics of Materials*, 2021, **152**.

1433 71. E. Dickinson, *Food Hydrocolloids*, 2012, **28**, 224-241.

1434 72. H. Koc, M. Drake, C. J. Vinyard, G. Essick, F. van de Velde and E. A. Foegeding, *Food*
1435   *Hydrocolloids*, 2019, **94**, 311-325.

1436 73. D. J. McClements, F. J. Monahan and J. E. Kinsella, *Journal of Texture Studies*, 1993, **24**,
1437   411-422.

1438 74. A. J. Gravelle, S. Barbut and A. G. Marangoni, *Rsc Advances*, 2015, **5**, 60723-60735.

1439 75. A. J. Gravelle, R. A. Nicholson, S. Barbut and A. G. Marangoni, *Food Research*
1440   *International*, 2019, **122**, 209-221.

1441 76. H. Khalesi, W. Lu, K. Nishinari and Y. P. Fang, *Food Chemistry*, 2021, **364**.

1442 77. A. J. Gravelle and A. G. Marangoni, *Food Hydrocolloids*, 2021, **119**.

1443 78. W. H. Shih, W. Y. Shih, S. I. Kim, J. Liu and I. A. Aksay, *Physical Review A*, 1990, **42**,
1444   4772-4779.

1445 79. Z. Y. Zhang, H. Pham, Y. B. Tan, H. L. Zhou and D. J. McClements, *Food Biophysics*,
1446   2021, **16**, 512-519.

1447 80. M. Felix, Z. Camacho-Ocana, M. L. Lopez-Castejon and M. Ruiz-Dominguez, *Food*
1448   *Hydrocolloids*, 2021, **120**.

1449 81. Y. D. Zhu, D. Li and L. J. Wang, *Powder Technology*, 2019, **358**, 95-102.

1450 82. K. D. Mattice and A. G. Marangoni, *Current Research in Food Science*, 2020, **3**, 59-66.

1451 83. R. G. M. van der Sman, P. Chakraborty, N. P. Hua and N. Kollmann, *Food Hydrocolloids*,
1452   2023, **135**.

1453 84. P. V. Gadkari, M. J. T. Reaney and S. Ghosh, *International Journal of Biological*
1454   *Macromolecules*, 2019, **126**, 337-344.

1455 85. K. M. Kamani, G. J. Donley, R. K. Rao, A. M. Grillet, C. Roberts, A. Shetty and S. A.
1456   Rogers, *Journal of Rheology*, 2023, **67**, 331-352.

1457 86. H. S. Joyner, in *Annual Review of Food Science and Technology, Vol 12, 2021*, eds. M.
1458   Doyle and D. J. McClements, 2021, vol. 12, pp. 591-609.

1459 87. H. S. Melito, C. R. Daubert and E. A. Foegeding, *Journal of Food Engineering*, 2012, **113**,
1460   124-135.

1461 88. F. K. G. Schreuders, M. Schlangen, I. Bodnar, P. Erni, R. M. Boom and A. J. van der Goot,
1462   *Food Hydrocolloids*, 2022, **124**.

1463 89. F. K. G. Schreuders, L. M. C. Sagis, I. Bodnar, P. Erni, R. M. Boom and A. J. van der Goot,
1464   *Food Hydrocolloids*, 2021, **110**.

1465 90. Y. X. Ma, J. L. Niu, D. Li and L. J. Wang, *International Journal of Food Engineering*, 2020,

1466   **16**.
1467 91. Y. X. Ma, D. B. Su, Y. Wang, D. Li and L. J. Wang, *Lwt-Food Science and Technology*,
1468   2020, **128**.
1469 92. J. Yu, X. Y. Wang, D. Li, L. J. Wang and Y. Wang, *Food Hydrocolloids*, 2022, **131**.
1470 93. G. Vu, H. L. Zhou and D. J. McClements, *Journal of Agriculture and Food Research*, 2022,
1471   **9**.
1472 94. H. L. Zhou, G. Vu, X. P. Gong and D. J. McClements, *Acs Food Science & Technology*,
1473   2022, **2**, 844-851.
1474 95. A. T. Noguerol, V. Larrea and M. J. Pagan, *European Food Research and Technology*,
1475   2022, **248**, 2483-2496.
1476 96. Q. B. Zhang, L. Huang, H. Li, D. Zhao, J. N. Cao, Y. Song and X. Q. Liu, *Molecules*, 2022,
1477   **27**.
1478 97. A. Bakhsh, S. J. Lee, E. Y. Lee, N. Sabikun, Y. H. Hwang and S. T. Joo, *Foods*, 2021, **10**.
1479 98. K. Uruc, A. Tekin, D. Sahingil and A. A. Hayaloglu, *Innovative Food Science & Emerging*
1480   *Technologies*, 2022, **82**.
1481 99. B. Cui, Y. Y. Mao, H. S. Liang, Y. Li, J. Li, S. X. Ye, W. X. Chen and B. Li, *International*
1482   *Journal of Biological Macromolecules*, 2022, **206**, 481-488.
1483